Using Geochemical Data and Aquifer Simulation to Characterize Recharge and Groundwater Flow in the Middle Rio Grande Basin, New Mexico

L. Niel Plummer and Ward E. Sanford

U.S. Geological Survey, Reston, Virginia

Laura M. Bexfield and Scott K. Anderholm

U.S. Geological Survey, Albuquerque, New Mexico

Eurybiades Busenberg

U.S. Geological Survey, Reston, Virginia

Chemical and isotopic data for groundwater from the Middle Rio Grande Basin, New Mexico, were used to (1) delineate hydrochemical zones and their source area to the basin, (2) evaluate paleo-recharge conditions, including recharge from the Rio Grande and mountain fronts, and (3) calibrate a basin-scale groundwater model. Twelve sources of recharge and one zone of groundwater discharge were identified and traced throughout the basin. Geochemical mass-balance calculations, accounting for mixing of surface-water and groundwater sources, evapotranspiration/dilution processes, and water-rock reaction, led to well-defined radiocarbon ages that range from modern to more than 30 ka B.P. in the Santa Fe Group aquifer system. Recharge rates determined from the groundwater model were appreciably lower than previous estimates based on a rainfall-runoff model, but in agreement with recharge estimates determined from a previous investigation using the chloride mass-balance method. The groundwater model reproduces key features of the groundwater-flow system, including a trough in the water-table surface in the central part of the basin, and accounts for the observation of a substantial quantity of paleo Rio Grande water in the aquifer. Results from a 30,000-year transient simulation suggest that recharge at the Last Glacial Maximum (LGM) may have been ten times the modern rate, but that recharge following the LGM was about 60 percent of the modern rate. Over the past 30 ka, δ^2H of Rio Grande water was maximum in the present and at about 15 ka, and minimum at approximately 5 ka and 22 ka, before present. Seasonal shifts in the timing of peak discharge of the Rio Grande and/or changes in the amounts of low-altitude

Groundwater Recharge in a Desert Environment:
The Southwestern United States
Water Science and Application 9

10.1029/009WSA11

precipitation along the basin margins and base flow to the Rio Grande may explain observed variations in the stable isotopic composition of paleo Rio Grande water.

INTRODUCTION

In the early 1990s, investigations of the hydrogeologic framework of the Santa Fe Group aquifer system in the vicinity of Albuquerque [*Hawley and Haase*, 1992] showed that the highly productive aquifer, from which the city of Albuquerque obtains its water supply, is much less extensive and thinner than previously was thought [*Bjorklund and Maxwell*, 1961; *Reeder et al.*, 1967]. A steady increase in groundwater pumping in the Albuquerque vicinity since about the mid-1940's has resulted in declines in water levels in excess of 36 m [*Bexfield and Anderholm*, 2002]. A series of investigations were conducted in the early 1990s to improve understanding of the geohydrologic framework and hydrologic conditions in the aquifer system in the vicinity of Albuquerque [*Thorn et al.*, 1993], and to incorporate the new information into improved versions of the USGS groundwater-flow model for the basin [*Kernodle et al.*, 1995; *Kernodle,* 1998].

In 1995, the U.S. Geological Survey (USGS), in cooperation with other Federal, State and local agencies, initiated a 6-year investigation of the geology and hydrology of the Middle Rio Grande Basin (MRGB) [*Bartolino and Cole,* 2002]. As a part of that overall investigation, extensive chemical and isotopic data, including radiocarbon and stable isotope data, were obtained for groundwater in the Santa Fe Group aquifer system of the MRGB. The objectives of the USGS hydrochemical study were to (1) identify sources of recharge to the basin and trace the flow of each source through the basin, (2) use the chemical and isotopic data to interpret paleorecharge conditions and improve the conceptual model of groundwater flow, and (3) use the radiocarbon data and improved conceptual model of groundwater flow to calibrate a groundwater-flow model and estimate modern and paleorecharge rates for the basin. This report summarizes some of the findings of the study, as they relate to recharge conditions in the semiarid Middle Rio Grande Basin. Further details of the investigation are given in *Plummer et al.* [2004], and *Sanford et al.* [2004].

Groundwater data were obtained from 288 wells and springs, and were supplemented with chemical data from the USGS National Water Information System (NWIS) and city of Albuquerque data bases. The data include major and minor-element chemistry (30 elements), oxygen-18 (^{18}O) and deuterium (^{2}H) content of water, carbon-13 (^{13}C) and carbon-14 (^{14}C) content of dissolved inorganic carbon (DIC), sulfur-34 (^{34}S) content of dissolved sulfate, tritium (^{3}H), and contents of selected dissolved gases (including dissolved oxygen (DO), nitrogen (N_2), argon (Ar), helium (He), chlorofluorocarbons (CFCs: CFC-11, CFC-12, CFC-113), and sulfur hexafluoride (SF_6)). The chemical and isotopic composition of surface waters in the basin were investigated and are given along with the groundwater data in *Plummer et al.* [2004], where details of sample collection and analysis, and specifics of the USGS study can be found.

MIDDLE RIO GRANDE BASIN

The Middle Rio Grande Basin of central New Mexico (Figure 1), also known as the Albuquerque Basin [*Anderholm*, 1988; *Thorn et al.,* 1993; *Kernodle,* 1998], covers about 7,900 km^2 and contains basin-fill deposits up to 4.2 km thick [*Thorn et al.,* 1993]. Mountains border the basin on the north, east, and southwest margins. The climate of the MRGB is semiarid, and average precipitation ranges from about 22 cm/year at Albuquerque (altitude 1,600 m) to about 58 cm/year along the crest of the Sandia Mountains (altitude 3,300 m) east of Albuquerque [*Bartolino and Cole,* 2002]. *Grissino-Mayer* [1995, 1996] used tree-ring records to show that the minimum and maximum average annual rainfall in an area located about 100 km west of the MRGB was 32.7 and 42.3 cm/year, respectively, over the past 2,129 years.

The Rio Grande, which extends the entire length of the basin (Figure 1), is the primary surface drainage. The headwaters of the Rio Grande are located in the San Juan Mountains of southwestern Colorado, which exceed 4,100 m in altitude [*Ellis et al.,* 1993]. Although the Rio Grande is the only perennial stream in the MRGB, at least ten ephemeral streams can contribute substantial flow to the Rio Grande, and possibly contribute substantial quantities of recharge to the underlying aquifer.

The MRGB is recharged from several sources [*Kernodle et al.,* 1995], including mountain-front recharge, subsurface groundwater inflow from adjacent basins, and seepage from the Rio Grande and ephemeral streams. Mountain-front recharge represents recharge to the MRGB from infiltration of flow from streams with headwaters in the mountainous area adjacent to the basin, and groundwater inflow from the mountainous area [*Anderholm,* 2001]. Other sources of recharge in the MRGB [*Anderholm*, 2001] include direct infiltration of precipitation to basin-fill deposits, infiltration

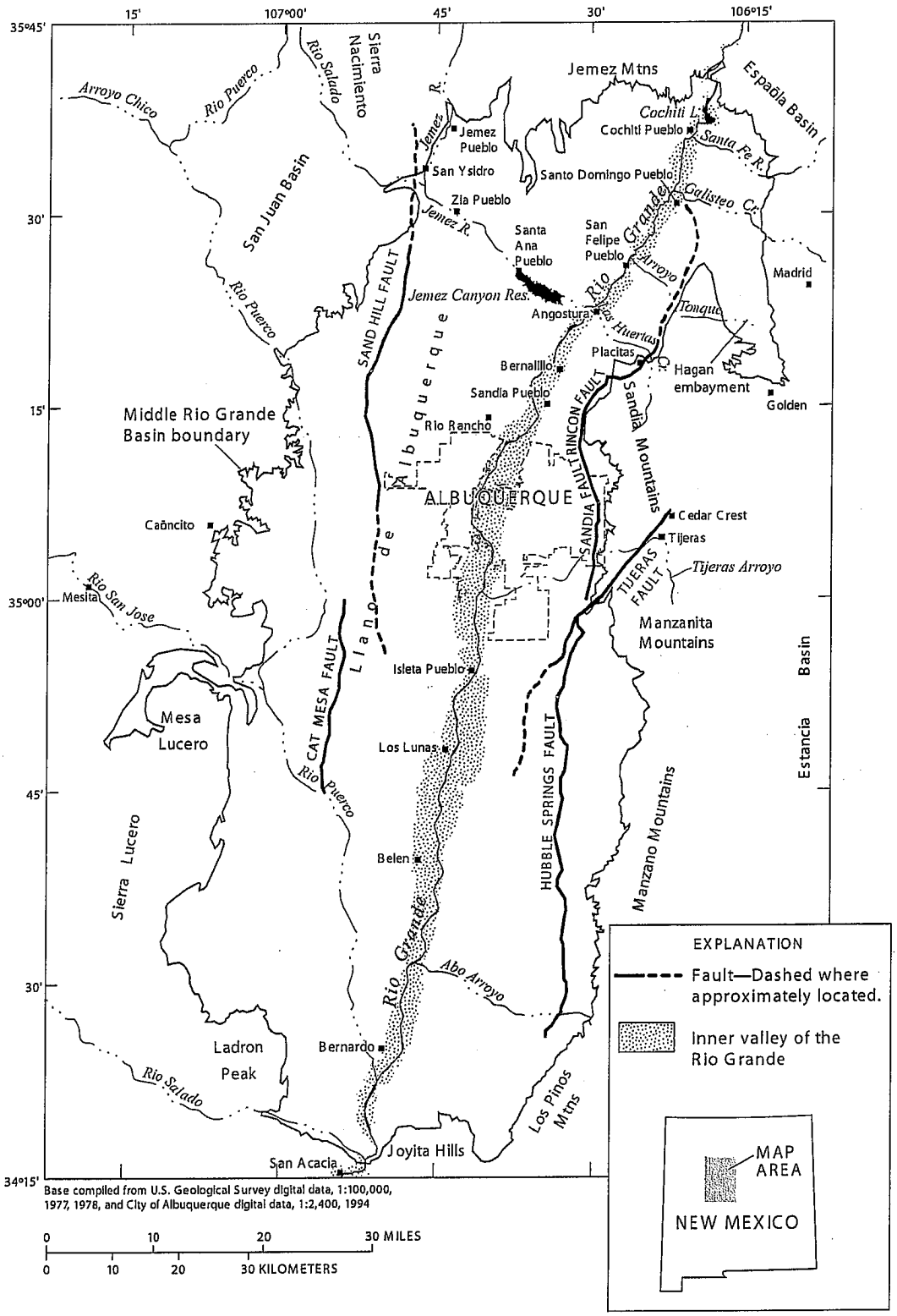

Figure 1. Selected features of the Middle Rio Grande Basin, New Mexico.

of runoff in arroyos with headwaters in the alluvial basin, and infiltration of water from perennial streams that cross the alluvial basin.

Groundwater discharges from the MRGB to the Socorro Basin near San Acacia (Figure 1). Groundwater discharge also occurs within the MRGB through evapotranspiration (particularly in the Rio Grande flood plain), and, today, through groundwater pumpage and into agricultural drains along some reaches of the Rio Grande.

Predevelopment water-level maps [*Titus*, 1961; *Bexfield and Anderholm*, 2000] show that groundwater flow through the central part of the basin has been oriented primarily north to south, whereas flow near the basin margins has been oriented toward the central part of the basin (Figure 2).

PATTERNS IN CHEMICAL AND ISOTOPIC COMPOSITION OF GROUNDWATER

Distinct spatial patterns in the chemical and isotopic composition of groundwater in the MRGB have been recognized and mapped throughout the basin [*Anderholm*, 1988; *Logan*, 1990; *Plummer et al.*, 2001, 2004]. In many cases, the patterns reflect unique chemical and/or isotopic signatures that are indicative of the water source and can be used to distinguish waters recharged along mountains at the basin margin from waters originating as seepage of surface water into the aquifer, or water originating as subsurface inflow from adjacent basins. The chemical and isotopic patterns are particularly useful in characterizing groundwater flow in the basin because geochemical reactions appear to be limited within the primarily siliciclastic aquifer; thus, the waters retain much of their source-water compositional signatures. Contour lines on the concentrations of most dissolved solutes align parallel to the predominant north to south direction of groundwater flow through the central part of the basin.

Major-Element Composition

Spatial patterns in specific conductance serve to demonstrate patterns observed in several of the major-element constituents of groundwater in the basin (Plate 1). The largest values of specific conductance (greater than 2,000 µS/cm) typically are near the western margin of the basin, where mineralized groundwater is believed to enter the basin as sub-surface inflow from Paleozoic and Mesozoic rocks to the west. Values of specific conductance greater than about 1,000 µS/cm also are observed near the Hagan embayment in the northeast part of the basin, near the Tijeras Fault Zone along the eastern margin, and at the southern end of the basin. The smallest values of specific conductance (less than 400 µS/cm) are along parts of the northern and eastern mountain fronts, and in an area extending across Rio Rancho and Albuquerque in the north-central part of the basin. Maps of the concentrations of many major and minor-element constituents in the MRGB are given in *Plummer et al.* [2004].

The most common water type is Ca-HCO_3, followed by Na-HCO_3 and mixed-cation-HCO_3. Different water types tend to group in distinct areas of the basin. Na generally is the dominant cation west of the Rio Grande (except near the northern end of the basin), whereas Ca generally dominates east of the Rio Grande. Mixed-cation samples are relatively common near the Rio Puerco, in the southeastern part of the basin, and in some parts of Albuquerque. HCO_3 is the dominant anion across much of the eastern and northern parts of the basin, whereas SO_4 dominates in areas near Abo Arroyo in the southeast part of the basin and the Hagan embayment to the northeast, as well as across much of the western part of the basin. The mixed-anion waters are relatively common west of the Rio Grande, whereas elevated Cl concentrations (above background levels) are primarily in the southwestern part of the basin.

Stable H and O Isotopic Composition of Groundwater

The stable isotopic composition of groundwater also can be contoured in the MRGB (Plate 2) and appears to be indicative of the source. The contours align north to south in the central part of the basin, parallel to the direction of the general north to south groundwater flow. A zone of isotopically depleted water (δ^2H typically < –90 per mil) extends throughout the central part of the basin. An area of isotopically enriched water (δ^2H typically > –80 per mil) occurs along the western and southwestern parts of the basin. The range of δ^2H values of all the water sampled outside the Albuquerque area is 65 per mil (–118.3 to –52.9 per mil), compared to 38 per mil (–111.3 to –73.7 per mil) in the Albuquerque area.

Along both sides of the Rio Grande, from about San Felipe Pueblo to the southern extent of the basin, is a zone of water with δ^2H values in the –90s per mil range, similar to that of modern Rio Grande. Rio Grande water is depleted in stable isotopic composition relative to the average local precipitation because the river contains runoff from high altitude precipitation and snowmelt from mountains in northern New Mexico and southern Colorado [*Yapp*, 1985]. Finally, water with δ^2H values in the –70s and –80s per mil range occurs along the eastern and northern margins of the basin (Plate 2).

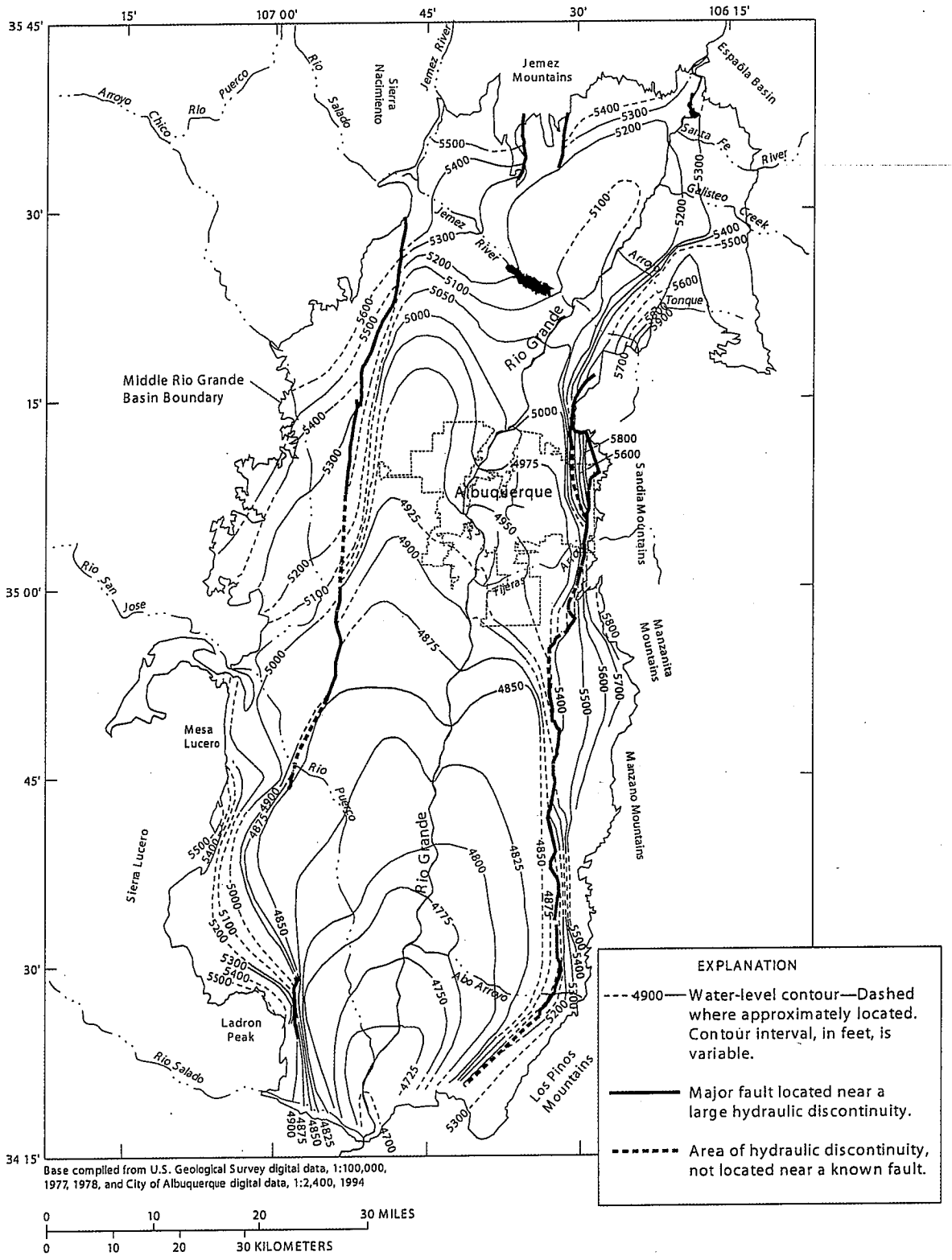

Figure 2. Predevelopment water levels in the Middle Rio Grande Basin. Contours in feet (1 foot=0.3048 meter) based on original source (Bexfield and Anderholm, 2000).

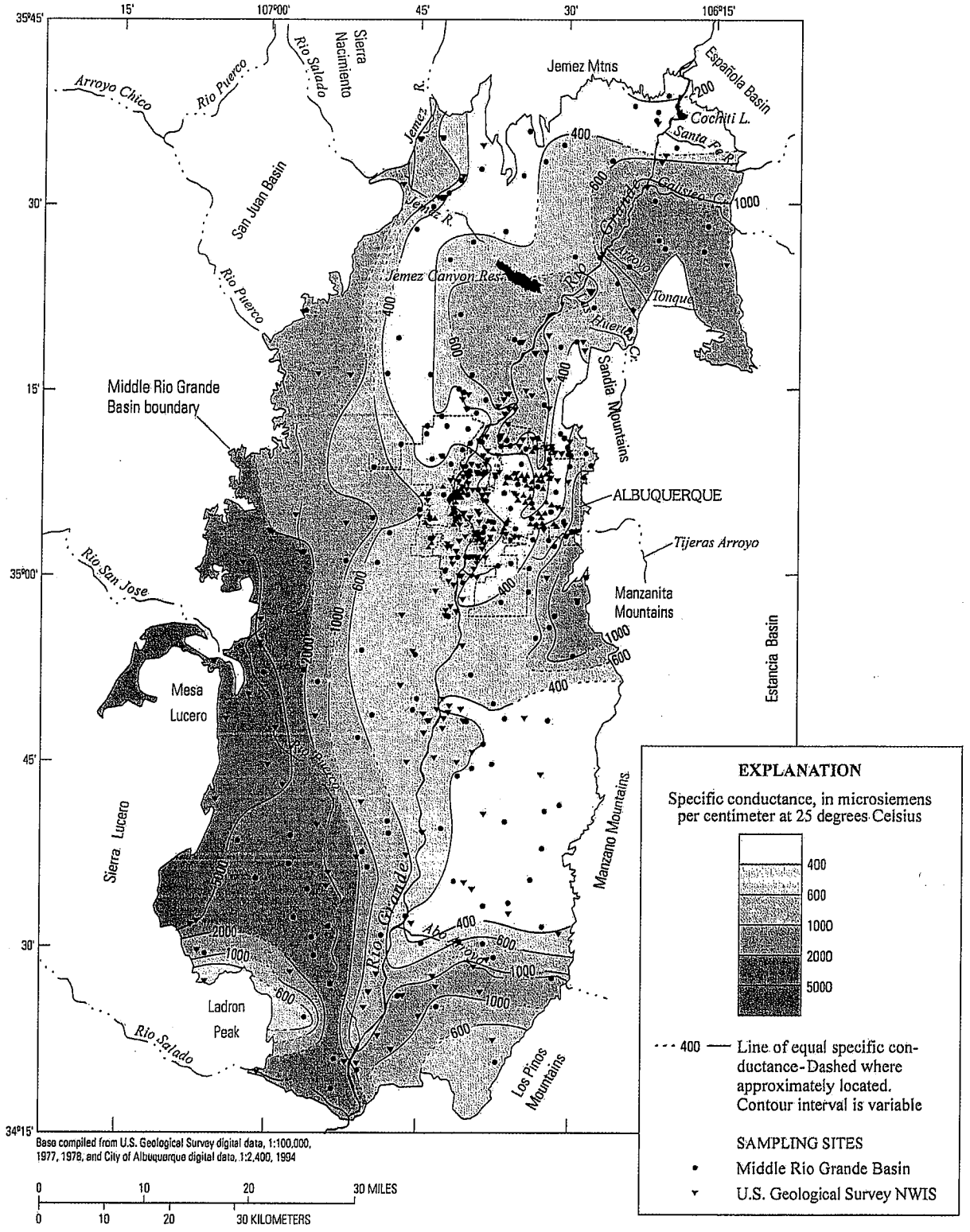

Plate 1. Specific conductance of groundwater of the Middle Rio Grande Basin.

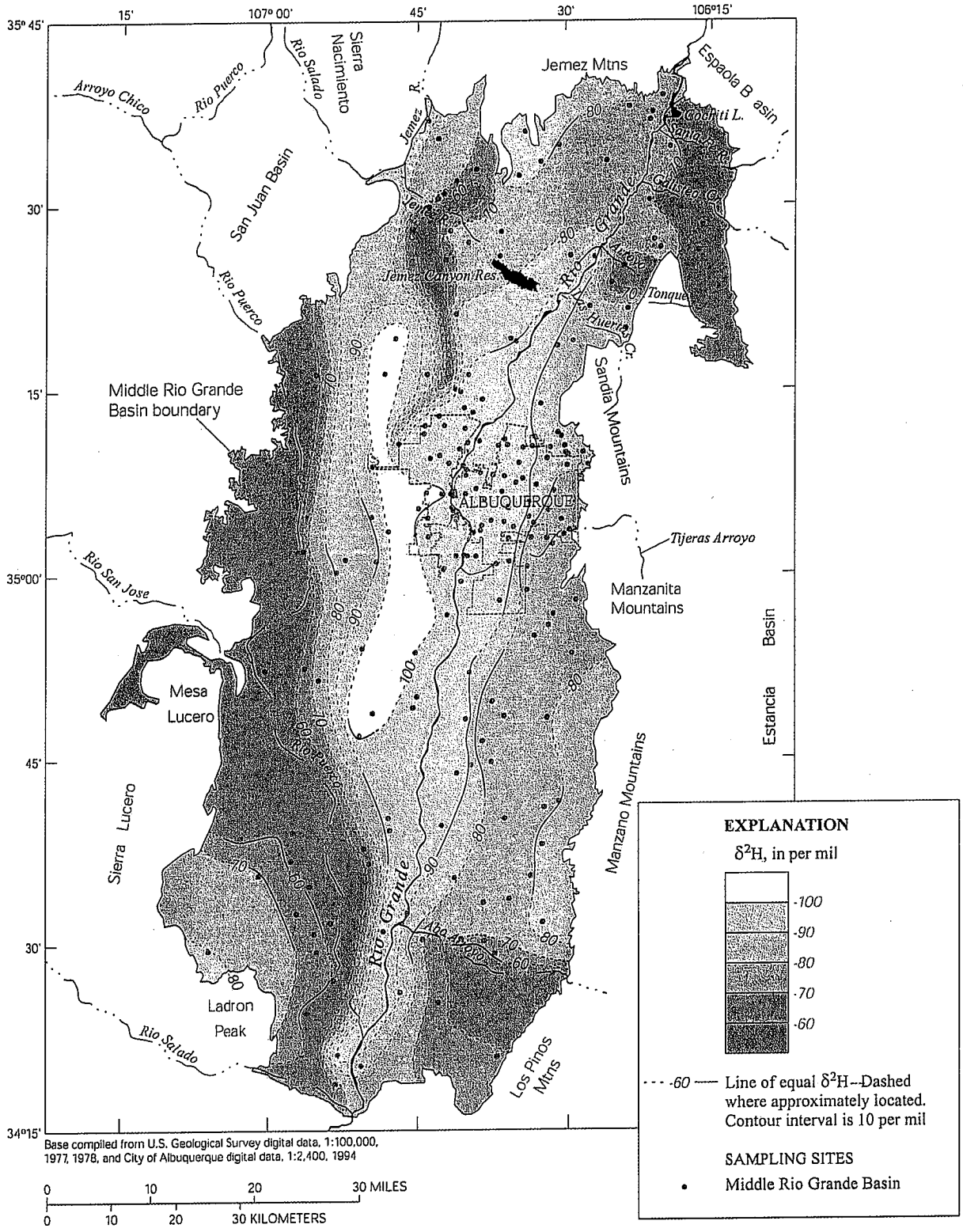

Plate 2. Variations in the δ^2H isotopic composition of groundwater throughout the Middle Rio Grande Basin.

Patterns in stable isotopic composition of water in the vicinity of Albuquerque were first recognized by *Yapp* [1985], and now are defined in greater detail over the entire MRGB. Groundwater along the eastern side of Albuquerque nearest the Sandia Mountains, referred to by *Yapp* [1985] as "Eastern domain" waters, consistently was enriched in ^2H (δ^2H of –75 to –86 per mil), and was attributed to recharge from precipitation that fell in the Sandia Mountains. Over a narrow transition striking north-northeast, and of horizontal width of only about 2 km, the δ^2H isopleths of groundwater at Albuquerque become distinctly depleted in ^2H, to a composition similar to that of the modern Rio Grande (Figure 3). Yapp [1985] referred to these depleted waters as "Western domain" waters, with δ^2H values of –90 to about -95 per mil, and suggested that they represented waters recharged by infiltration of Rio Grande water. Within the "Western domain" waters, *Yapp* [1985] recognized a third group of waters on the west side of the Rio Grande, southwest of Albuquerque, that were even more depleted than modern Rio Grande water; these waters were referred to by Yapp as "Deuterium-depleted Deep water", with δ^2H values observed by *Yapp* [1985] of –102 to –104 per mil. *Yapp* [1985] suggested that the "Deuterium-depleted Deep water" was recharged from the Rio Grande at a time when the river was on average about 10 per mil more depleted in ^2H than at present. However, as shown by *Plummer et al.* [2004], the "Deuterium-depleted Deep water" can be traced to the northern margin of the basin and probably represents recharge that occurred along the flanks of the Jemez Mountains north of the MRGB during the last glacial period. The "Deuterium-depleted Deep water" of *Yapp* [1985] clearly is not of Rio Grande origin.

The sharp boundary between mountain-front recharge (δ^2H values in the –80s per mil) and Rio Grande water (δ^2H values in the –90s per mil) found at Albuquerque (Figure 3) appears to extend north through Sandia Pueblo to San Felipe Pueblo, where the depleted Rio Grande stable isotope signal pinches out at the Rio Grande. The stable isotope pattern is consistent with the suggestion of *Yapp* [1985] that, north of San Felipe, there is net discharge of groundwater to the Rio Grande, but further south from San Felipe, there is net loss of Rio Grande water to the aquifer. Based on stable isotope data, the zone of influence of infiltration from the Rio Grande is more than approximately 15 km in width just north of Albuquerque, remains about 15 km wide through most of Albuquerque, and then narrows south of Albuquerque parallel to the Rio Grande (Plate 2). Waters with stable isotopic composition similar to the Rio Grande appear to mix with other western, northern, and eastern sources of water in the southernmost part of the basin, and/or discharge to the Rio Grande.

Tritium and Chlorofluorocarbons

Nearly all groundwater samples were analyzed for chlorofluorocarbons, and tritium measurements were made in about half of the groundwater samples. Tritium and chlorofluorocarbon measurements were used to identify water samples that were recharged approximately post-1950 (for tritium) and post-1940 (for chlorofluorocarbons), or to identify water samples that contain fractions of post-1950 or post-1940 recharge, respectively. Tritium concentrations were near values for modern (1995) precipitation (10–12 TU) in groundwater samples located along the eastern margin of the basin (eastern mountain front). Groundwater samples containing more than 0.2 TU always contained detectible concentrations of chlorofluorocarbons, especially CFC-12. The mountain-front groundwater samples containing significant concentrations of tritium also contained 130 to 1,100 pg/kg of CFC-12. Therefore, in the absence of tritium measurements, chlorofluorocarbons provided similar information to that obtained from tritium pertaining to young-water fractions. CFC-12 and tritium were detected routinely in groundwater along the mountain-front margin of the basin, in groundwater from the inner valley of the Rio Grande, and near some arroyos. The absence of CFC-12 and/or tritium provided a useful criteria for screening water samples in which the ^{14}C activity had not been contaminated with ^{14}C from atmospheric testing of nuclear bombs.

^{14}C Activity in Groundwater

The measured ^{14}C activities of DIC of groundwater from 211 sites in the MRGB range from 0.62 to 123.1 percent modern carbon (pmC). Patterns in the ^{14}C activity of the DIC can be mapped throughout the basin (Plate 3). Most of the contours in ^{14}C activity align in a north-south direction that roughly parallels the water source. ^{14}C activities are highest along the eastern mountain front, along the northern margin of the basin, and along the inner valley of the Rio Grande, corresponding to areas where recharge has most likely occurred in the past 5–10 ka. Relatively high ^{14}C activities also occur near areas where Abo Arroyo, the Rio Puerco, and the Jemez River enter the basin (Plate 3). Waters with low values of ^{14}C activity of the DIC are present along the western and southwestern basin margins. A zone of low ^{14}C activity extends through nearly the entire length of the west-central part of the basin.

HYDROCHEMICAL ZONES

Using the chemical and isotopic composition of MRGB groundwater, 12 separate zones of recharge to the basin

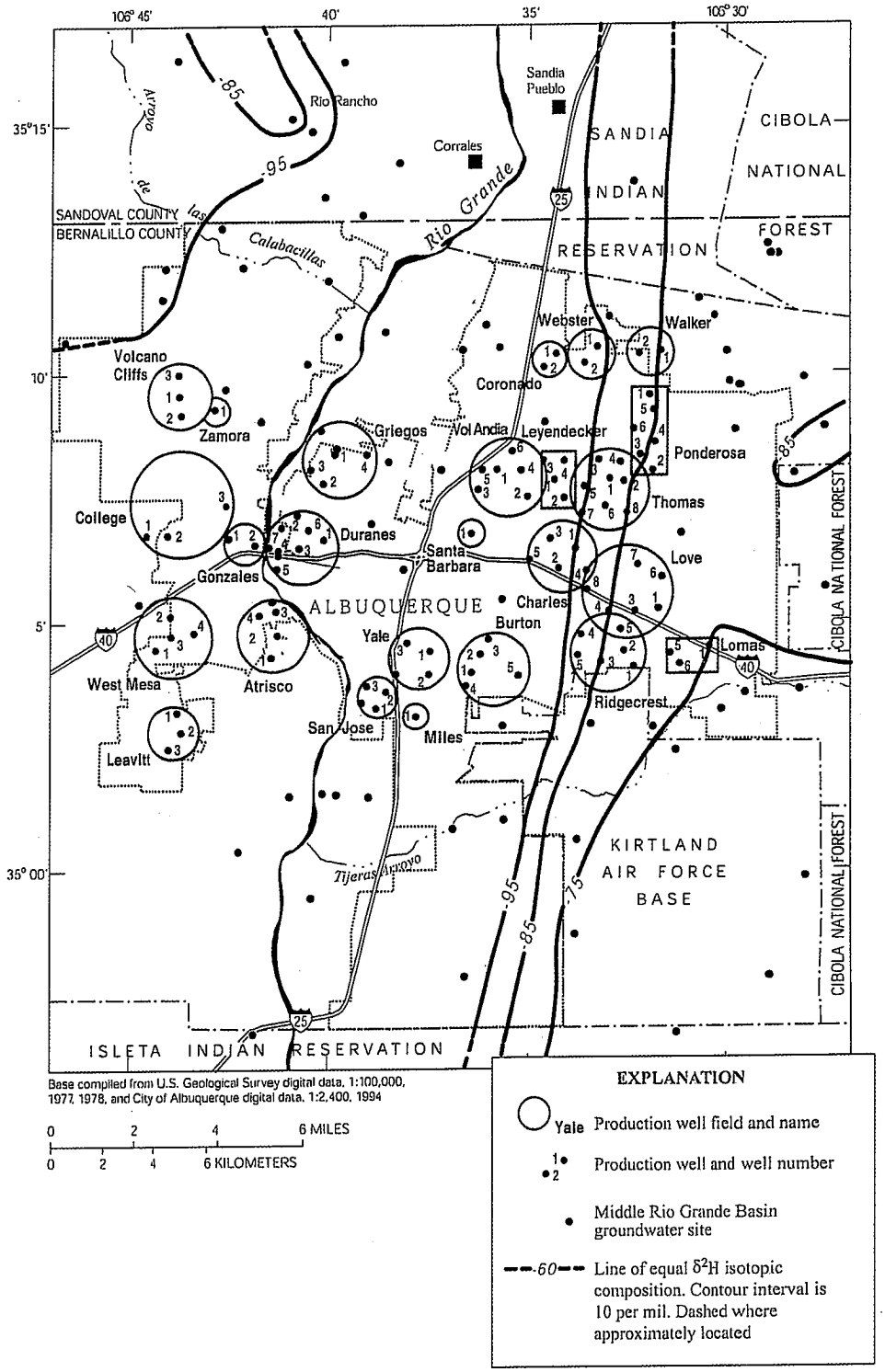

Figure 3. Variations in δ^2H isotopic composition of groundwater in the vicinity of Albuquerque. Circles and boxes identify production well fields. The closely spaced contours on the east side of Albuquerque mark the boundary between the Eastern Mountain Front zone (to the east) and the Central zone (to the west).

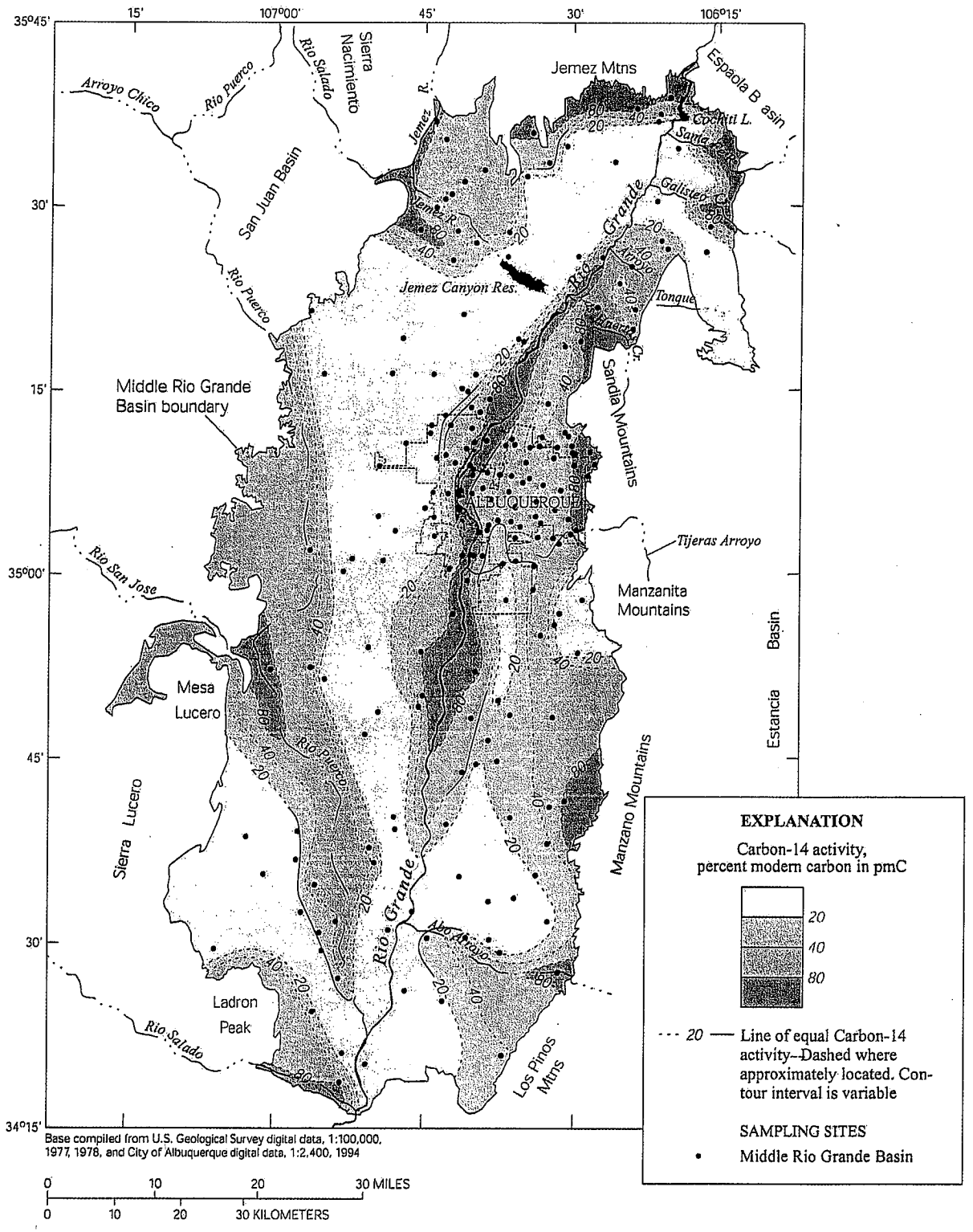

Plate 3. Variations in ^{14}C activity (pmC) for dissolved inorganic carbon from groundwater throughout the Middle Rio Grande Basin.

(Figure 4) and a zone of groundwater discharge were recognized [*Plummer et al.*, 2001, 2004]. The hydrochemical zones and median values of selected chemical and isotopic parameters for each zone are listed in Table 1. The separation of each hydrochemical zone from adjacent zones was supported by a Mann-Whitney statistical test [*Plummer et al.*, 2004]. The hydrochemical zones provide insight into likely recharge sources, flow paths, and aquifer properties.

Mountain front recharge is the predominant source of water to the Northern Mountain Front, Eastern Mountain Front, and Southwestern Mountain Front zones (Figure 4). Comparison of the basin-averaged Cl concentration in precipitation (0.21 mg/L, Table 2) with Cl concentration in groundwater indicates that most groundwater samples originating as mountain-front recharge were concentrated by factors of 16- to more than 100-fold during recharge, as a result of evapotranspiration. The data of *Anderholm* [2001] lead to a similar result for evapotranspiration during groundwater recharge along the eastern mountain front.

Groundwater in the Northwestern zone (Figure 4) is attributed to recharge in areas along the southern edge of the Jemez Mountains and to localized infiltration through the Jemez River. The Cl data from the Northwestern zone indicate samples that have been concentrated up to about 60-fold during recharge, although one sample appears to contain elevated Cl concentration from infiltration of Jemez River water or upward leakage of deep mineralized water. Five of the eleven samples from the Northwestern zone, including samples from wells more than 240 m deep, have NO_3 concentrations of higher than 5 mg/L (as N). These samples fall along the precipitation evaporation trend for NO_3 versus Cl concentration, and contain fairly high dissolved-oxygen concentrations, which is consistent with a natural source of NO_3. Compared with adjacent hydrochemical zones, the enriched ^2H content of most groundwater in the Northwestern zone (Table 1) indicates that recharge occurred at relatively low altitude along the Jemez Mountains.

Potential sources of groundwater recharge to the West-Central zone (Figure 4) include mountain-front recharge and, possibly, groundwater inflow from north of the basin. The West-Central zone extends from the base of the Jemez and Nacimiento Mountains (at depth beneath the Northwestern zone) in the northwestern part of the MRGB (Figure 4), and can be traced south through much of the western portion of the basin between the Rio Puerco and the Rio Grande to the vicinity of the Rio Grande south of Belen (Figure 1). In some areas, the zone also may extend under the Rio Grande to the east side of the basin at depth, accounting for the "Deuterium-Depleted Deep Water" of *Yapp* [1985], but the full extent of this zone is not known in detail (Figure 4). Based on the Cl concentration of precipitation, most groundwater samples in the West-Central zone appear to have been concentrated between about 8- and 270-fold during recharge. High-altitude parts of the Jemez Mountains appear to be the most likely recharge area that could explain depleted ^2H content and low ^{14}C activity (long travel times—thousands of years) of water in the West-Central zone, although the possibility of a recharge area even farther north of the MRGB cannot be ruled out completely.

The Western Boundary zone (Figure 4) includes groundwater inflow from Mesozoic to Paleozoic rocks west of the basin and local arroyo recharge. Water in the Rio Puerco zone (Figure 4) probably includes infiltration through the Rio Puerco and groundwater inflow from Mesozoic and (or) Paleozoic rocks along the western margin of the basin. Groundwater of the Abo Arroyo zone (Figure 4) probably originates as infiltration of surface water through Abo Arroyo, groundwater inflow from the Abo Arroyo watershed, and mountain-front recharge. Sources of recharge associated with the Tijeras Fault Zone (Figure 4) include mountain-front recharge along the Manzanita Mountains and inflow of deep groundwater across the eastern basin margin. Potential sources of recharge to the Tijeras Arroyo zone are the infiltration of surface water through the arroyo and groundwater inflow from the Tijeras Arroyo watershed. Mountain-front recharge also is likely to contribute a portion of the water recharging this zone. Potential sources of recharge to the Northeastern zone include groundwater inflow from adjacent areas, including the Hagan embayment, the infiltration of surface water through arroyo channels, and, possibly, mountain-front recharge, particularly in the southern part of the zone.

Water in the Central zone (Figure 4) is attributed primarily to infiltration of Rio Grande water. The Central zone stretches along the Rio Grande from San Felipe Pueblo (Figure 1) in the north to just north of Abo Arroyo in the southern part of the basin (Figure 4). The depleted ^2H content of groundwater in the Central zone relative to that of Eastern Mountain Front water (Table 1) indicates infiltration through the Rio Grande, and not local precipitation, as the primary source of recharge. The Cl concentrations (Tables 1 and 2) indicate that the median groundwater sample from the Central zone is concentrated by a factor of 1.8 relative to the historical, discharge-weighted, Rio Grande water composition (Table 2), with a maximum concentration factor attributed to evapotranspiration for some samples from the inner valley of the Rio Grande of nearly 8-fold.

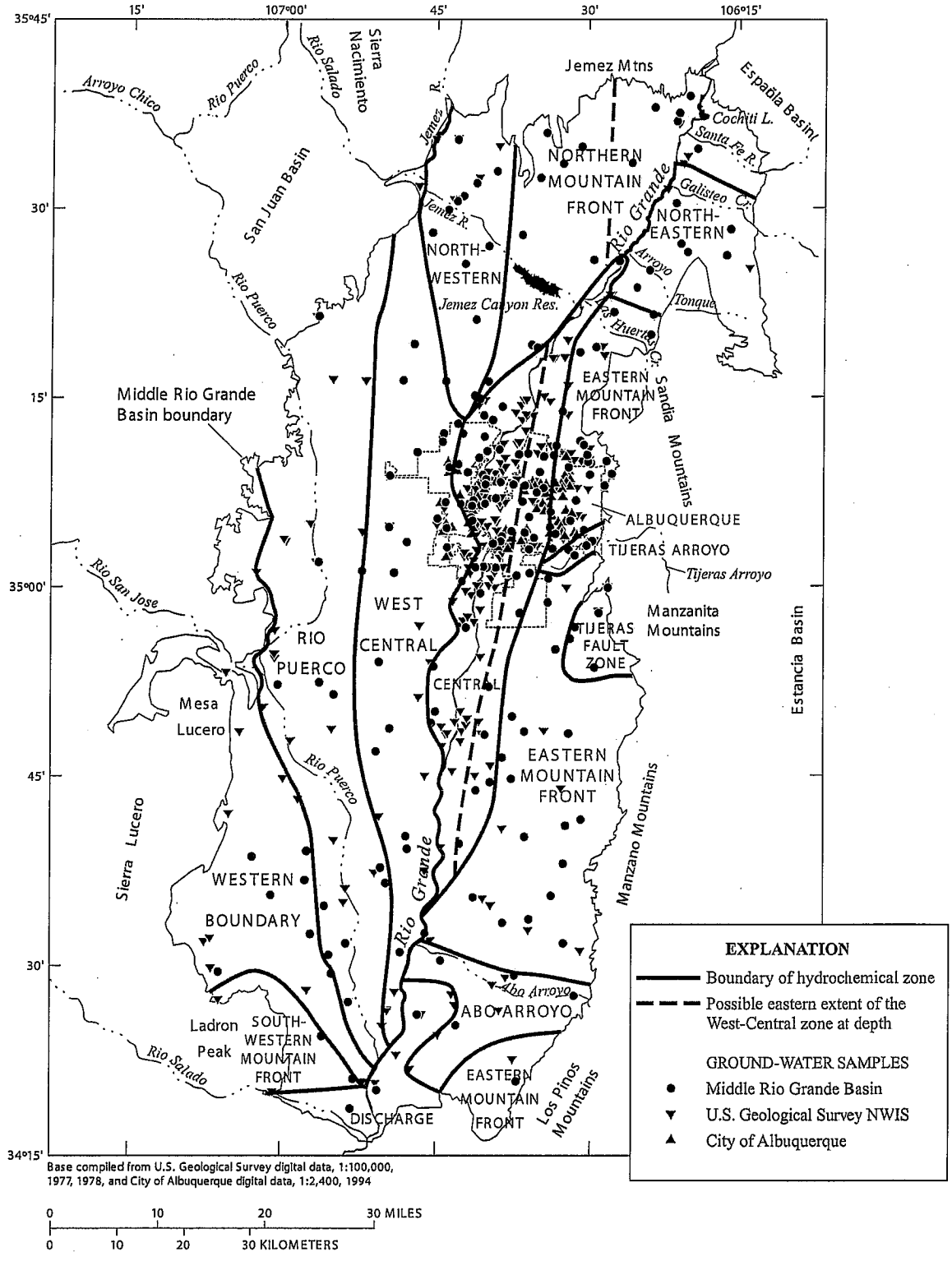

Figure 4. Hydrochemical zones defined for the Middle Rio Grande Basin. The dashed lines represent the possible extent of the West-Central zone at depth beneath other zones.

Table 1. Median values of selected water-quality parameters by hydrochemical zone[a,b,c]

Hydrochemical Zone	Spec. Cond. (µS/cm)	pH	Water Temp. (°C)	DO	Ca	Mg	Na	K	Alk.	SO_4	Cl	F	Br	SiO_2	NO_3	Al	As
NMF[e]	340	7.49	18.9	5.12	38.5	6.1	20.0	4.9	137.	19.5	5.6	0.35	0.08	53.3	0.56	—	3.2
Northwestern	400	7.84	20.6	6.68	33.9	4.2	49.9	5.7	160.	44.8	8.5	0.61	0.07	30.1	2.44	—	9.8
West Central	535	8.22	23.8	3.00	12.0	2.5	103.	4.2	174.	92.0	13.4	0.99	0.11	34.5	1.24	6.76	23.2
Western Boundary	4,572	7.70	22.0	4.09	135.	56.4	589.	15.2	300.	793.	820.	1.64	0.38	22.5	0.86	5.00	1.8
Rio Puerco	2,731	7.50	20.0	3.73	135.	42.7	290.	10.4	190.	1,080.	185.8	0.63	0.64	21.8	0.88	5.00	1.0
SWMF[e]	462	8.11	19.1	4.43	52.6	13.5	27.8	2.5	202.	53.0	15.0	1.02	0.21	17.6	1.12	3.31	0.2
Abo Arroyo	1,055	7.45	20.7	6.23	92.5	34.4	49.2	3.1	148.	346.	25.9	0.90	0.17	24.0	1.40	4.14	5.2
EMF[e]	382	7.67	22.0	5.16	45.0	5.1	29.2	2.2	157.	31.0	10.5	0.60	0.17	28.4	0.31	5.56	2.0
Tijeras Fault Zone	1,406	7.42	18.5	4.66	171.	36.0	95.0	6.1	599.	100.	139.	1.27	0.69	18.9	1.09	5.22	2.2
Tijeras Arroyo	677	7.39	16.1	6.97	89.4	24.5	29.3	3.8	240.	115.	56.6	0.60	0.35	19.5	3.79	4.09	1.0
Northeastern	1,221	7.50	19.4	6.44	141.	29.5	81.8	4.8	208.	390.	22.7	0.51	0.19	38.5	0.64	4.34	2.7
Central	436	7.74	18.1	0.12	42.9	8.0	31.0	6.4	158.	66.0	16.6	0.44	0.09	47.0	0.08	6.00	5.4
Discharge	1,771	7.70	20.6	0.08	93.0	31.0	190.	10.5	157.	290.	280.	1.40	0.47	39.0	0.42	4.50	9.9

Table 1. (continued)

Hydrochemical Zone	Ba	B	Cr	Cu	Fe	Pb	Li	Mn	Mo	Sr	U	V	Zn	δD (‰)	$\delta^{18}O$ (‰)	$\delta^{13}C$ (‰)	^{14}C (pmC)	^{14}C Age[d] (ka)
NMF[e]	0.062	0.043	1.2	0.8	0.060	0.20	0.058	0.005	1.7	0.31	1.0	6.4	258.	-77.7	-10.9	-8.50	33.4	8.8
Northwestern	0.056	0.118	2.0	0.4	0.030	0.10	0.068	0.002	3.4	0.57	2.7	15.6	9.0	-64.7	-8.73	-6.93	29.6	9.8
West Central	0.032	0.239	5.7	0.5	0.028	0.11	0.045	0.002	8.2	0.20	3.7	27.9	5.0	-96.7	-12.7	-7.18	8.80	19.5
Western Boundary	0.014	0.900	10.6	3.0	0.213	0.12	0.251	0.041	9.9	2.09	4.4	5.7	118.	-64.4	-9.12	-4.70	6.19	22.3
Rio Puerco	0.014	0.291	3.0	3.4	0.130	0.10	0.253	0.015	7.0	3.92	6.0	3.4	117.	-61.6	-8.51	-7.65	36.4	8.1
SWMF[e]	0.045	0.094	1.9	9.3	0.030	0.41	0.041	0.007	3.0	0.86	0.9	1.0	252.	-53.5	-7.74	-5.76	40.0	7.4
Abo Arroyo	0.017	0.130	4.4	2.0	0.105	0.10	0.031	0.004	3.4	1.48	5.4	9.5	8.1	-65.2	-9.05	-6.72	24.1	11.4
EMF[e]	0.084	0.050	1.0	1.7	0.031	0.27	0.020	0.003	2.0	0.32	3.6	7.5	6.7	-81.0	-11.4	-8.70	47.2	6.0
Tijeras Fault Zone	0.046	0.347	1.7	4.3	0.111	0.34	0.227	0.023	3.7	1.11	7.3	6.3	61.5	-74.2	-10.3	-0.98	9.70	18.7
Tijeras Arroyo	0.057	0.060	1.1	1.0	0.050	0.10	0.017	0.005	1.9	0.47	3.7	3.0	4.5	-75.7	-10.3	-6.80	72.8	2.6
Northeastern	0.018	0.215	3.2	3.7	0.170	0.11	0.040	0.004	6.7	1.72	8.5	3.8	99.5	-68.6	-9.72	-6.40	28.5	10.1
Central	0.083	0.085	1.0	0.8	0.041	0.10	0.040	0.015	5.0	0.40	3.6	9.3	5.0	-95.4	-12.8	-8.87	61.0	4.0
Discharge	0.030	0.630	10.2	1.7	0.080	0.15	0.326	0.010	10.3	3.02	3.9	7.1	16.2	-90.8	-12.1	-7.00	10.8	17.9

[a]—, no data; µS/cm, microsiemens per centimeter at 25 degrees Celsius; °C, degrees Celsius; ‰, per mil; pmC, percent modern carbon.

[b]Concentrations in milligrams per liter, mg/L: DO, dissolved oxygen; Ca, calcium; Mg, magnesium; Na, sodium; Alk., titration alkalinity as HCO_3; SO_4, sulfate; Cl, chloride; F, fluoride; Br, bromide; SiO_2, silica as SiO_2; NO_3, nitrate as N; Ba, barium; B, boron; Fe, iron; Li, lithium; Mn, manganese; Sr, strontium.

[c]Concentrations in micrograms per liter, µg/L: Al, aluminum; As, arsenic; Cr, chromium; Cu, copper; Pb, lead; Mo, molybdenum; U, uranium; V, vanadium; Zn, zinc.

[d]Median of years. Unadjusted radiocarbon age, Libby half-life, in thousands.

[e]NMF, Northern Mountain Front; SWMF, Southwestern Mountain Front; EMF, Eastern Mountain Front.

Water from the Southwestern, Western Boundary, Rio Puerco, West-Central, Central, Eastern Mountain Front, and Abo Arroyo zones probably discharges to the Rio Grande or to the Socorro Basin to the south at the southern tip of the MRGB (Figure 4).

MASS-BALANCE CALCULATIONS

Geochemical mass-balance calculations were made using NETPATH [*Plummer et al.*, 1994] to obtain estimates of the amounts of various sources of water to the basin, and to investigate the possible effects of geochemical reactions on the radiocarbon ages. Although water from each hydrochemical zone is characterized according to its primary source, most groundwater samples in the MRGB contain small fractions of waters from other sources, such as upward leakage of saline waters, infiltration from nearby surface-water sources, or inflow from adjacent basins. Detailed examination of the hydrochemical data [*Plummer et al.*, 2004] indicates that many groundwater samples also have been affected by evapotranspiration or dilution, and geochemical reactions to varying extents.

Table 2. Summary of chemical and isotopic properties of source waters for the Middle Rio Grande Basin[a,b]

Source	pH	DO[c]	Alk.	Ca	Mg	Na	K	Cl	SO_4	SiO_2	$\delta^{13}C$ (‰)[c]	^{14}C (pmC)[c]
Precipitation												
Sevilleta	5.4	nd	1.7	0.94	0.09	0.12	0.15	0.21	1.40	nd	-8.0	100
Precipitation with ET of 8-Fold												
PRECIPx8	5.4	8.0	0.525[d]	7.5	0.7	1.0	1.2	1.7	11.2	nd	-8.0	100
Mountain-Front Recharge[												
NMF	7.4	8.0	124	29	3.9	16	4.3	4.4	14	53	-12.0	100
EMF	7.4	8.0	212	61	7.5	16	1.6	6.4	31	23	-12.0	100
SWMF	7.3	8.0	207	54	12.0	19	1.3	12.0	33	29	-12.0	100
Ground-Water Inflow												
NEGW	7.5	0.0	328	67	15.0	67	5.0	27.0	63	13	-4.0	2
SWGW	7.7	0.0	2,073	474	230	6,069	143	7,202	5,020	21	-4.0	2
ASSP	6.7	7.4	1,180	607	513	5,910	149	8,070	3,750	17	2.8	8
MWGW	7.7	0.0	1,366	300	145	3,532	117	2,700	3,250	21	-4.0	2
Upward Leakage of Saline Waters												
Saline 1	7.0	0.1	182	185	26	1530	107	2,520	296	43	-7.5	23
Saline 2	6.5	2.8	1305	322	70	382	44	581	140	17	-0.6	5
Surface Waters												
RP	8.0	1.0	183	138	29	200	7.0	46	707	10	-0.1	64
RGA	8.1	8.0	118	37	6.4	22	3.0	9.2	58	19	-7.5	100
RGSF	8.1	8.0	112	35	6.3	17	2.6	4.8	50	18	-7.5	100
JRW	8.1	8.0	129	39	4.6	62	5.5	50	79	22	-2.9	83
ABO	8.3	8.0	254	297	105	123	1.5	61	1,049	19	-7.1	87
TIJ	8.2	8.0	243	102	21	39	5.5	82	105	16	-7.1	87
GAL	8.1	8.8	220	150	45	140	3.7	23	630	17	-6.0	100
LUC	6.8	nd	536	171	57	131	5.4	46	183	18	-5.0	100

[a]Sevilleta, [*Moore, 1999,* Precipitation chemistry data on the Sevilleta National Wildlife Refuge, 1989-1995 (http://sevilleta.unm.edu/research/local/nutrient/precipitation/#data)]; PRECIPx8, Sevilleta with evapotranspiration (ET) factor of 8-fold; NMF, Northern Mountain Front, median; EMF, Eastern Mountain Front, median; SWMF, Southwestern Mountain Front, NWIS, representative sample; NEGW, Northeast Groundwater inflow, NWIS, representative sample; SWGW, Southwest Groundwater Inflow, NWIS, median; ASSP, Arroyo Salado Spring; MWGW, Mid-West Groundwater Inflow, NWIS, median; Saline 1, mineralized upward leakage from Domestic Well #04, NM041; Saline 2, mineralized upward leakage from Coyote Spring, NM031; RP, discharge-weighted average NWIS Rio Puerco at Bernardo; RGA, discharge-weighted average NWIS Rio Grande at Albuquerque; RGSF, discharge-weighted average NWIS Rio Grande at San Felipe; JRW, discharge-weighted average NWIS Jemez River below Jemez Canyon Dam; ABO, median Abo Arroyo; TIJ, discharge-weighted average NWIS Tijeras Arroyo above Four Hills Road; GAL, Galisteo Creek above reservoir, June 1974; LUC, Lucero-24, Los Alamos National Laboratory, representative of southwest arroyo water; nd, no data. NMxxx numbers refer to sample numbers from Plummer et al. (2004).

[b]Concentrations in milligrams per liter, mg/L: DO, dissolved oxygen; Alk., titration alkalinity as HCO_3; Ca, calcium; Mg, magnesium; Na, sodium; K, potassium; Cl, chloride; SO_4, sulfate; SiO_2, silica as SiO_2; ‰, per mil; pmC, percent modern Carbon.

[c]Estimated.

[d]mg/l as CO_2.

In constructing the geochemical mass-balance models, each groundwater sample in the MRGB was assumed to have evolved from a primary source-water composition, and, subsequently, was altered to varying degrees by:

- Evapotranspiration/dilution processes,
- Mixing with surface water(s),
- Mixing with saline upward leakage water(s),
- Mixing with groundwater inflow from adjacent basins
- Water/rock reaction.

Compositions of the primary source waters and compositions of secondary waters that may mix with primary source waters in the basin are summarized in Table 2. In many

cases, the chemical compositions of the source waters represent averages of sample compositions from the USGS NWIS surface-water database, or in the cases of "ASSP", "Saline Water 1" and "Saline Water 2", the compositions are those of individual samples collected as a part of this investigation (see Table 2). Details of the calculations are given in *Plummer et al.* [2004].

The average calculated percentages of various source waters in samples from each hydrochemical zone are summarized in Table 3. Most waters recharged along the basin-margin mountain-front (Northern Mountain Front, Northwestern, West Central, Southwestern Mountain Front, and Eastern Mountain Front zones) contain typically more than 90-percent mountain-front source water that has mixed with generally small fractions of saline upward leakage water (Table 3). The fractions of "Saline Water 1" were lowest in the Northwestern and Southwestern zones, and averaged 1.5, 0.7, and 1.0 percent in the Northern Mountain Front, West Central, and Eastern Mountain Front zones, respectively. Water samples from the Western Boundary and Rio Puerco zones contain on average 7.8 and 7.4 percent, respectively, of groundwater inflow from sources along the western margin of the basin. Water samples in the Rio Puerco zone contain an average of 92.6 percent Rio Puerco water. Water samples from the Abo Arroyo zone were found to be predominantly of Eastern Mountain Front origin mixed with an average of 28 percent Abo Arroyo water. Water from the Central Zone was almost entirely of Rio Grande origin, averaging 99.6 percent water of Rio Grande origin, which was mixed with "Saline Water 1". Waters from the Tijeras Fault Zone and Tijeras Arroyo were found to be fairly complex mixtures of Eastern Mountain Front water with varying fractions of Tijeras Arroyo water and "Saline Waters 1 and 2". Water samples from the Northeastern zone were complex mixtures of Eastern Mountain Front water, Northeast Groundwater inflow, surface water from Galisteo Creek, and "Saline Water 1" (Table 3).

RADIOCARBON AGES OF DISSOLVED INORGANIC CARBON

The geochemical mass-balance calculations using NETPATH indicate that, in most cases, there is net precipitation of small amounts of calcite through most of the MRGB. This precipitation of calcite does not appreciably alter the ^{14}C content. The exception is the West-Central zone, where small amounts of calcite dissolve in association with small relative increases in Ca/Na cation exchange. The net calcite mass transfer is near zero in other parts of the basin (Northern Mountain Front, Northwestern, and Central zones). Small amounts of plagioclase feldspar weathering also were found throughout the MRGB. Gypsum essentially is absent in most of the MRGB sediment, except in parts of the Western Boundary and Rio Puerco zones, where the

Table 3. Summary of predominant groundwater sources by hydrochemical zone[a]

Zone no.	Hydrochemical zone	Primary water	Percent range of primary water	Average percent of primary water	Secondary water	Percent range of secondary water	Average percent of secondary water	Additional water	Percent range of additional water	Average percent of additional water
1	NMF	NMF	92.3–100	98.5	Saline 1	0–7.3	1.5			
2	Northwestern	NMF	97.1–100	99.9	Saline 1	0–2.9	0.1			
3	West Central	NMF	92.5–100	99.3	Saline 1	0–7.5	0.7			
4	Western Boundary	LUC	84.0–100	92.2	ASSP	0–16.0	7.8			
5	Rio Puerco	RP	77.6–100	92.6	MWGS or SWGW	0–22.4	7.4			
6	SWMF	SWMF	100	100.0	Saline 1	0	0.0			
7	Abo Arroyo	EMF	47.7–100	72.1	ABO	0–52.3	27.9			
8	EMF	EMF	89.5–100	99.0	Saline 1	0–10.5	1.0			
9	Tijeras Fault Zone	EMF	61.2–100	89.5	Saline 1,2	0–38.8	10.5			
10	Tijeras Arroyo	EMF	2.9–92.3	61.6	TIJ	9.1–91.6	37.4	Saline 2	0–6.6	1.6
11	Northeastern	EMF	14.2–98.9	66.3	NEGW, GAL	1.1–85.8	33.4	Saline 1	0–2.0	0.3
12	Central	RGA	96.5–100	99.6	Saline 1	0–3.5	0.4			

[a]NMF, Northern Mountain Front; Saline 1, NM041; RP, average discharge-weighted NWIS Rio Puerco; RGA, average discharge-weighted NWIS Rio Grande at Albuquerque; MWGW, Mid-West Groundwater Inflow; SWGW, Southwest Groundwater Inflow; SWMF, Southwestern Mountain Front, NWIS; EMF, Eastern Mountain Front, median; ABO, median Abo Arroyo; Saline 2,- Coyote Spring, NM029; TIJ, average discharge-weighted NWIS Tijeras Arroyo; NEGW, Northeast Ground Water Inflow; GAL, Galesteo Creek above reservoir, used as arroyo source in hydrochemical zone 11. NMxxx numbers refer to sample numbers from Plummer et al. (2004).

calculated mass of gypsum dissolution is higher than in other hydrochemical zones. The small differences in gypsum mass transfer outside of the Western Boundary and Rio Puerco zones probably reflect, at least in part, uncertainty in the calcium sulfate content of source waters to the MRGB. Redox reactions were considered only in the Central zone, where anoxic conditions are present in the inner valley of the Rio Grande. Here, the NETPATH models found, on average, a net oxidation of 0.28 mmol/L of organic carbon.

In most cases, the adjusted radiocarbon age from NETPATH was nearly identical to the unadjusted radiocarbon age, indicating that geochemical reactions do not appreciably affect the calculated ages. Therefore, the unadjusted radiocarbon age was adopted, and referred to as radiocarbon age below.

The radiocarbon ages in Plate 4 apply to water in the upper approximately 60 m of the Santa Fe Group aquifer system. The youngest water (0–2 ka) is along the mountain-front basin margins (east, northeast, and southwest margins of the basin), and along parts of the Rio Grande and Rio Puerco. Radiocarbon ages of 0–10 ka are along nearly the entire reach of the Rio Grande, the Rio Puerco, Galisteo Creek, Tijeras Arroyo, and Abo Arroyo, associated with relatively recent surface-water infiltration. The oldest waters are in the West-Central zone, the Western Boundary zone, and parts of the Eastern Mountain Front zone, as well as throughout the Discharge zone (Plate 4).

The median radiocarbon age of DIC in groundwater from 275 analyses throughout the MRGB, excluding samples contaminated with post-bomb ^{14}C, is 8.1 ka, with a range of approximately 0 to more than 50 ka. In the mountain-front hydrochemical zones, the median radiocarbon age is, for the Northern Mountain Front, Northwestern, Southwestern Mountain Front, and Eastern Mountain Front zones, 8.8, 9.8, 7.4, and 5.2 ka, respectively. Water in the West-Central, Western Boundary, and Discharge zones has median radiocarbon ages of 19.5, 22.3, and 17.9 ka, respectively. Groundwater dominated by river/arroyo sources has median radiocarbon ages of 8.1, 4.0, and 2.6 ka for the Rio Puerco, Central, and Tijeras Arroyo zones, respectively. The median radiocarbon ages of DIC in water from the Abo Arroyo, Tijeras Fault Zone, and Northeastern zones are 11.4, 18.7, and 10.1 ka, respectively. Further details are given in *Plummer et al.* [2004].

RETRIEVAL OF ENVIRONMENTAL AND CLIMATIC INFORMATION FROM RADIOCARBON AGES, STABLE ISOTOPE AND DISSOLVED GAS DATA

Having recognized water samples with a common source of recharge, the stable isotope, dissolved gas, and ^{14}C data permit interpretation of recharge conditions in parts of the MRGB. Here we examine and contrast recharge that originated as infiltration of Rio Grande water (Central zone) with water originating via mountain-front recharge (Eastern Mountain Front zone), and waters apparently originating as infiltration at relatively high altitude (greater than 2,500 m) along the flanks of the Jemez Mountains (West-Central zone), as a function of radiocarbon age over the past approximately 25 ka.

Recent paleoclimatic studies from New Mexico and the southwest U.S. provide a general framework for evaluating isotopic and dissolved gas data from the MRGB. Recharge temperatures determined from measurements of noble gases in groundwater from the Carrizo aquifer (Texas) and the San Juan Basin (northwestern New Mexico) indicated that the mean annual temperatures were 5.2 ± 0.7 and 5.5 ± 0.7 °C lower, respectively, during the Last Glacial Maximum (LGM) (approximately 18 ka radiocarbon years B.P.) than during the Holocene [*Stute et al.*, 1992; *Stute et al.*, 1995]. *Phillips et al.* [1986] found depletion of some 25 per mil in δ^2H of Pleistocene-age water relative to modern waters from the central San Juan Basin, northwestern New Mexico, and an average cooling of 5 to 7 °C during the last glacial period. *Thompson et al.* [1999] reconstructed estimates of annual temperature and annual precipitation in the vicinity of Yucca Mountain, southern Nevada, from studies of packrat middens for four intervals of the late Pleistocene. For the periods of 35–30 ka, 27–23 ka, 20.5–18 ka, and 14–11.5 ka, mean annual temperature was lower than today by about 4, 5, 8, and 5.5 °C, respectively, and mean annual precipitation was estimated to be 1.5, 2.2, 2.4, and 2.6 times modern levels of precipitation, respectively. Lake Estancia, to the east of the MRGB, had nine high stands from about 22 ka to 12 ka [*Allen and Anderson*, 2000]. The high stands of Lake Estancia record the pluvial of the last glacial period that occurred throughout the southwestern United States [*Benson et al.*, 1990; *Oviatt et al.*, 1992, *Phillips et al.*, 1992; *Wilkins and Currey*, 1997; *Allen and Anderson*, 2000].

Stable Isotope Records

The changes in δ^2H of water from the Central and Eastern Mountain Front zones during the past 5 ka are small, but vary in opposite direction as a function of radiocarbon age (Figure 5). During the past 5 ka, δ^2H of water from the Central zone (Rio Grande origin) increased by nearly 6 per mil from a minimum near –98 per mil; and δ^2H of moisture recharged along the Eastern Mountain front became more depleted in ^2H, by about 7 per mil (Figure 5). Most groundwater samples from the Eastern Mountain Front, with radio-

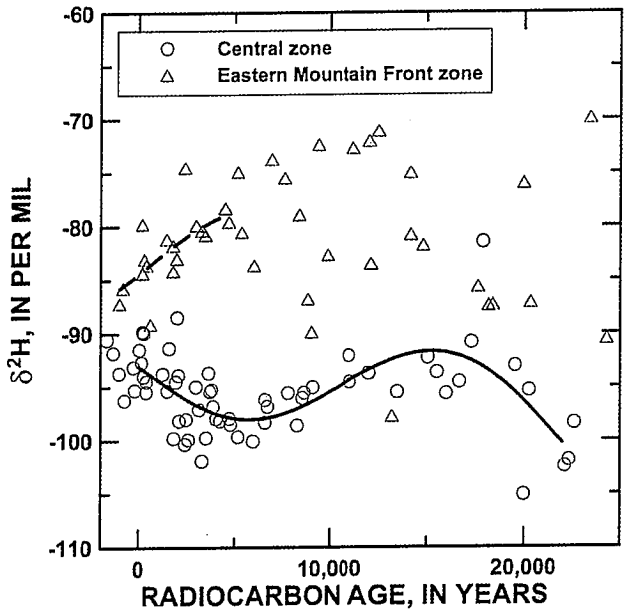

Figure 5. Comparison of δ^2H in groundwater from the Central zone with water recharged along the Eastern Mountain Front as a function of radiocarbon age. The lines represent polynomial fits to the data.

carbon ages greater than 5 ka B.P., range in δ^2H isotopic composition from about –90 to –70 per mil with little evidence of temporal variability (Figure 5). Water recharged from the Rio Grande to the Central zone apparently had a minimum δ^2H isotopic composition at approximately 5 ka B.P., reached a maximum at about 15 ka B.P., but was relatively depleted in ^2H at about 22 ka B.P. (Figure 5).

Today, δ^2H of Rio Grande water varies with season, and is, at least in part, affected by the extent of winter snow pack in southern Colorado and northern New Mexico [*Yapp*, 1985; *Plummer et al.*, 2004], and runoff from within the drainage basin. During the summer and fall, Rio Grande water becomes enriched in ^2H (Figure 6), reaching values of δ^2H of approximately –85 per mil in August through October of 1998 [*Plummer et al.*, 2004]. The enriched values probably are representative of base flow from the Rio Grande drainage basin mixed with runoff of low-altitude (less than 1,800 m) precipitation from the summer thunderstorms.

The depleted stable isotope values for Rio Grande water at about 20–28 ka B.P. (Figure 5) are consistent with cooling during the last glacial period and high proportions of water from snowmelt in the Rio Grande. At first inspection, the rest of the stable isotope record for paleo Rio Grande water seems inconsistent with paleo-climatic evidence. Specifically, Rio Grande water was enriched in ^2H during the relatively cold pluvial period from about 18 to 12 ka, and depleted in ^2H during the mid-Holocene warm period (4–8 ka B.P.) (Figure 5).

Two scenarios were considered to explain the historical variability in the δ^2H isotopic composition of Central zone groundwater: 1) variability in amounts of isotopically enriched low-altitude precipitation and base flow delivered to the Rio Grande, and 2) changes in the timing of peak runoff of snowmelt from northern New Mexico and southern Colorado. Both scenarios would vary the proportions of depleted high-altitude snowmelt and low-altitude runoff and base flow in Rio Grande discharge.

In the first scenario, dry climatic periods would lead to less runoff of low-altitude precipitation in the basin and less base flow to the Rio Grande. As a result, the Rio Grande would contain higher fractions of snowmelt and lower fractions of low-altitude precipitation and base flow, resulting in water that is relatively depleted in ^2H. Periods of relatively enriched ^2H isotopic composition of Rio Grande water would result from times of increased low-altitude precipitation in the basin and increased base flow to the Rio Grande. Consequently, the stable isotope record from the Central zone (Figure 5) would indicate increased low-altitude precipitation in the basin and increased base flow during the last pluvial, from about 18 to 12 ka B.P. and similarly, during the past approximately 5 ka. The relatively depleted stable isotopic composition of Central zone water from the mid-Holocene warm period, approximately 4–8 ka B.P., would indicate a period of decreased low-altitude precipitation in

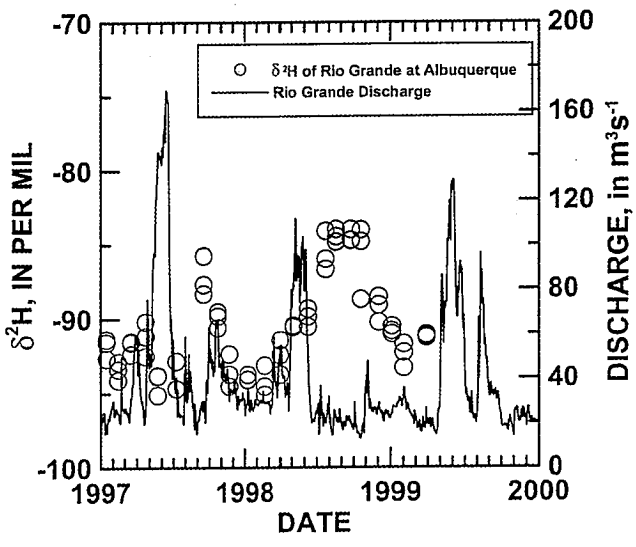

Figure 6. Seasonal variations in δ^2H of Rio Grande water at Albuquerque, 1997–99, in relation to discharge of the Rio Grande at Albuquerque, in cubic meters per second (m^3s^{-1}).

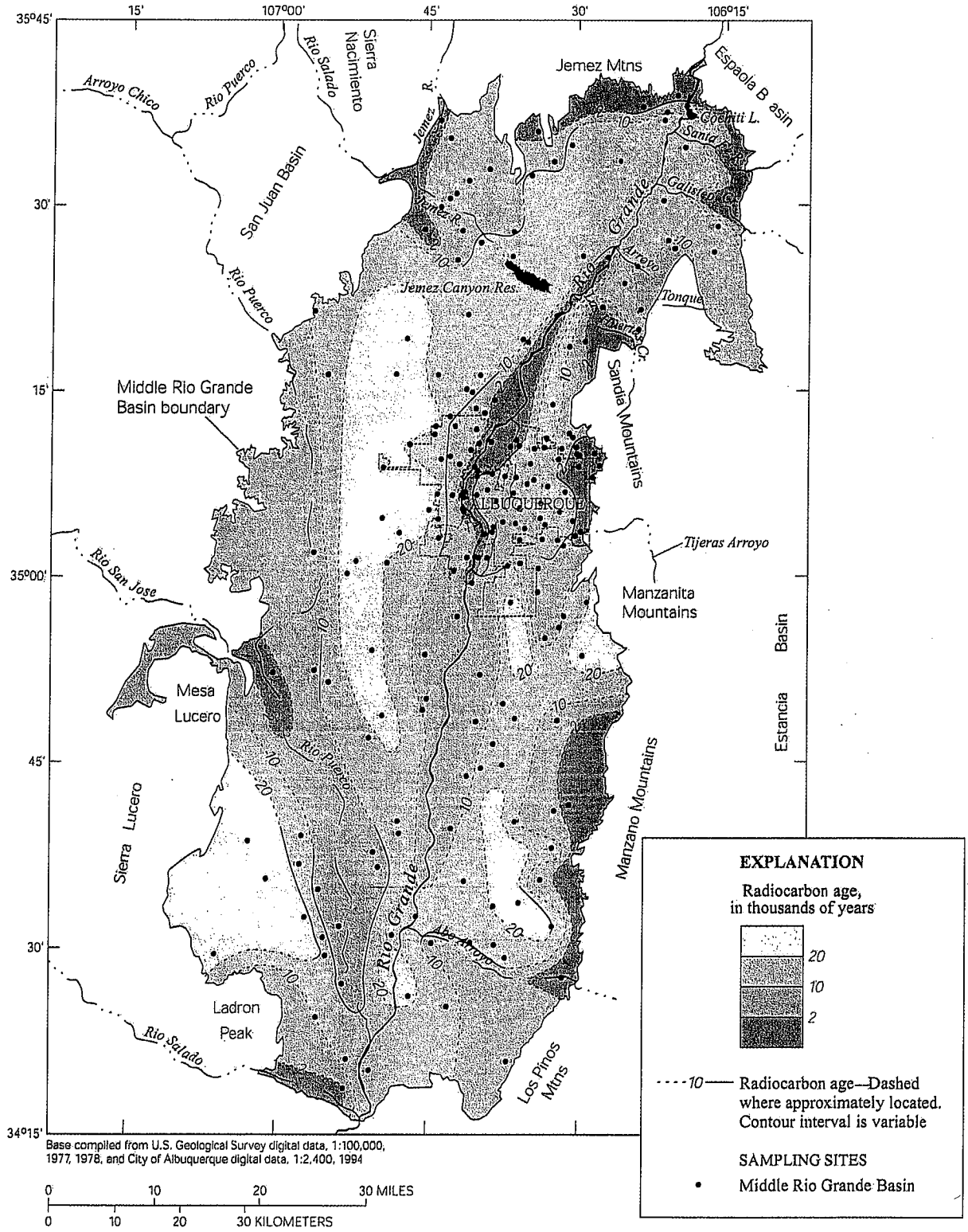

Plate 4. Variations in the unadjusted radiocarbon age (Libby half-life) of DIC in groundwater for the Middle Rio Grande Basin.

the basin and decreased base flow to the Rio Grande. This argument pertains only to the fractions of low- and high-altitude moisture sources in Rio Grande discharge, and not to historical variations in the magnitude of river discharge.

The second scenario recognizes that the timing of the spring snowmelt in the mountains of southern Colorado and northern New Mexico shifts with changes in seasonal temperature [*Cayan et al.*, 2001]. During the last glacial period, colder temperatures delayed the spring snowmelt and delayed the season of peak spring runoff. A cooling of 5 °C during the LGM may have caused periods of peak runoff of snowmelt to overlap, at least in part, with the summer thunderstorm season, resulting in an increase in the fraction of low-altitude summer precipitation mixed with mountain snowmelt. The resulting isotopic composition of the Rio Grande during peak runoff would be enriched in ^2H relative to that of snowmelt. During warm climatic periods, mountain snowmelt would occur in early spring and likely peak prior to the summer thunderstorm season, as it does today, resulting in peak runoff of the Rio Grande that is appreciably more depleted in ^2H than in cold times when snowmelt is delayed. This scenario implies that recharge to groundwater of the Central zone occurs primarily during periods of high discharge of the Rio Grande.

On the basis of the available data, neither of the two scenarios for explaining the historical variations in the isotopic composition of Central zone groundwater can be eliminated, and it is possible that, to some extent, both processes have contributed to the isotopic composition of water of Rio Grande origin.

Water Temperatures and Paleorecharge Temperatures

Throughout the MRGB, most groundwater temperatures are appreciably warmer than the modern mean annual air temperature at Albuquerque (13.6 °C). Warm ground temperatures in the MRGB result from heating under the influence of the local geothermal gradient [*Reiter*, 2001]. Median groundwater temperatures vary by hydrochemical zone from 16.1 °C (water in the Tijeras Arroyo zone) to 23.8 °C (water in the West-Central zone) (Table 1). Maximum water temperatures are about 30 °C for some water on the West Mesa, west of Albuquerque. The lowest water temperatures are found in shallow water samples at relatively high altitude, for example, discharge from Embudo and Embudito springs along the eastern mountain front above Albuquerque (altitudes of 2,012 and 1,963 m, respectively) has water temperatures of 8–9 °C.

In arid and semi-arid environments, recharge can occur (if at all) as continuous, diffuse infiltration of water through relatively deep unsaturated zones, maintaining close contact with the unsaturated zone air, or, as transient, focused recharge in response to, for example, floods in arroyos or stream valleys that bypass most water contact with the unsaturated-zone air [*Gee and Hillel,* 1988]. Therefore, water may partially or fully equilibrate with the unsaturated zone air (during diffuse-flow recharge), resulting in warm recharge temperatures calculated from dissolved gas data, or retain dissolved gas concentrations acquired at the land surface prior to recharge (during focused recharge), resulting in relatively cold recharge temperatures calculated from the dissolved gas data.

Recharge temperatures calculated from dissolved gas data [*Heaton and Vogel,* 1981; *Heaton et al.*, 1983; *Busenberg et al.,* 1993; *Stute and Schlosser*, 1999] appear to be biased warm in many waters from the MRGB [*Plummer et al.*, 2004]. If a paleoclimate signal remains in the calculated recharge temperatures, it will be found primarily in the samples with the lowest recharge temperatures for each hydrochemical zone. Samples with warm recharge temperatures have likely exchanged gases during infiltration through a thick unsaturated zone where temperatures can be greater than the local mean annual air temperature because of the geothermal gradient.

A most likely recharge altitude was assumed for each hydrochemical zone in calculation of recharge temperatures from the dissolved N_2-Ar data. Uncertainty of ± 450 m in recharge altitude results in an uncertainty of ± 2 °C in recharge temperature. Recharge temperatures were calculated for assumed recharge altitudes of 1,524, 1,981, or 2,438 m [*Plummer et al.*, 2004]. As the altitude of the Rio Grande is near 1,524 m, no water in the basin is recharged at altitudes lower than about 1,524 m. The upper extent of the range in recharge altitude (2,438 m) used in the calculation of recharge temperature corresponds to the higher altitudes along the eastern mountain front, and, in comparison with calculations based on other recharge altitudes, provides a means of estimating the dependence of the calculated recharge temperature on recharge altitude.

Eastern Mountain Front and West-Central zones. Recharge temperatures for water samples from the West-Central zone and the Eastern Mountain Front zone are compared with the measured water temperature in Figure 7. The recharge temperatures for waters from the West-Central zone were calculated assuming a recharge altitude of 2,438 m and those from the Eastern Mountain Front zone were calculated for recharge at 1,981 m. A relatively large range in recharge temperature is indicated, from about 3 to 22 °C for waters from the West-Central zone and about 8–18 °C

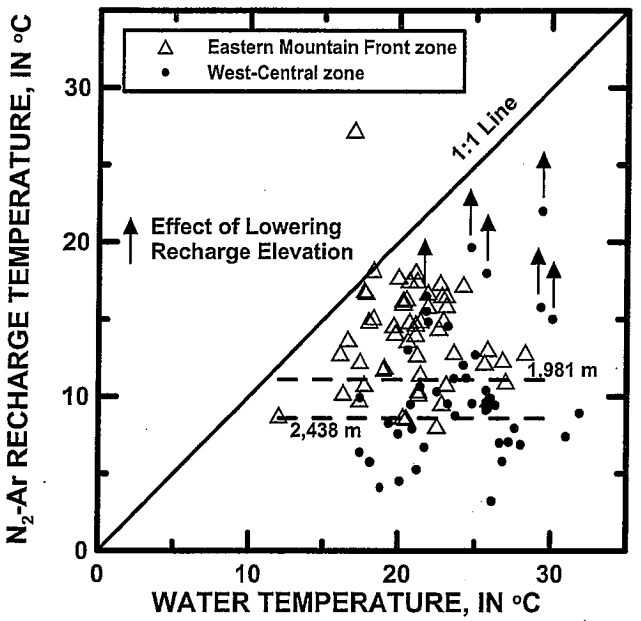

Figure 7. Comparison of N_2-Ar recharge temperature with the measured groundwater temperature for waters from the West-Central and Eastern Mountain Front zones. The arrows show the effect on the calculated recharge temperature if a lower altitude of recharge is assumed in the calculation. The recharge temperatures were calculated assuming altitudes of 1,981 m for the Eastern Mountain front and 2,438 m for the West-Central zone waters, respectively. The dashed lines show the estimated modern mean annual temperature for altitudes of 1,981 and 2,438 m.

for waters from the Eastern Mountain Front zone. The observed ranges in recharge temperatures are considerably larger than the range resulting from uncertainty in recharge altitude. Points plotting nearest the 1:1 line (Figure 7) indicate groundwater with calculated recharge temperatures similar to the measured water temperature, as would be expected in recharge that still is near the water table in the area where infiltration occurred. Most samples have water temperatures that are appreciably warmer than the calculated recharge temperature, indicating warming in the aquifer following recharge.

Assuming an average lapse rate of about -5.5 °C/km [*Meyer*, 1992], and the mean annual temperature of 13.6 °C at Albuquerque (altitude approximately 1,524 m), recharge temperatures of about 11.1 and 8.6 °C would be expected for water recharged at 1,981 and 2,438 m, respectively, today. A cooling of 5 °C in the mean annual temperature at the LGM [*Stute et al.*, 1992, 1995] could lead to recharge temperatures of 3–4 °C for higher-altitude recharge along the flanks of the Jemez Mountains (2,438 m), some 20 ka B.P., and recharge temperatures of about 6 and 9 °C at altitudes of 1,981 and 1,524 m, respectively, during the LGM.

Recharge temperatures in many West-Central zone waters are lower than the estimated modern mean annual temperature (8.6 °C at 2,438 m), and indicate recharge at altitudes higher than 2,438 m (barometric pressure lower than that at 2,438 m, and mean annual temperature lower than 8.6 °C), or recharge that occurred during the last glacial period, when mean annual temperature would have been lower than that observed today. Some waters from the West-Central zone apparently were recharged near 4 °C, if the recharge altitude was near 2,438 m (Figure 7). Similarly, waters from the Eastern Mountain Front zone with recharge temperatures lower than 11.1 °C indicate recharge at altitudes higher than 1,981 m, where mean annual temperature would be lower than 11.1 °C and barometric pressure would be lower than that at 1,981 m, or recharge during the last glacial period, when mean annual temperature would be lower than that observed today.

Other waters from the West-Central and Eastern Mountain Front zones were recharged at temperatures appreciably warmer than the paleo and modern mean annual temperature (Figure 7). These samples may indicate recharge by diffuse infiltration through a relatively thick unsaturated zone. The arrows on Figure 7 indicate that the calculated recharge temperatures for some samples from the West-Central zone would be closer to the 1:1 line if the samples were recharged at an altitude lower than 2,438 m, such as would be the case for samples recharged below thick unsaturated zones.

Central zone. Where the Santa Fe Group aquifer system and surface-water source are in contact, seepage from the surface-water source can pass directly into the aquifer system, and for those samples, the calculated recharge temperature probably represents the surface-water temperature at the time of recharge. Paleowater from the Central zone (of Rio Grande origin) has recharge temperatures that range from 8.9 to 18.4 °C.

Over the radiocarbon age spans of 15–27 ka, 11–13 ka, 5–9 ka, and 0–5 ka B.P., the average of values of recharge temperature for waters from the Central zone are 12.7 ± 1.4, 13.3 ± 1.5, 14.5 ± 1.4, and 13.0 ± 2.2 °C, respectively. The number of samples in each age range differ and the uncertainties represent one standard deviation of the mean.

During the period June 1996–March 1999, 74 monthly measurements of the temperature of Rio Grande water at six sites near Albuquerque [*Plummer et al.*, 2004] averaged 13.9 ± 7.6 °C, which is near the modern mean annual temperature at Albuquerque of 13.6 °C and within the range of the N_2-Ar recharge temperatures calculated for all of the paleowaters of Rio Grande origin, 12.7 ± 1.4 to 14.5 ± 1.4 °C. Today, Rio Grande water temperatures are maximum in

late July (near 25 °C) and minimum in early January (near 0 °C). Using the modern seasonal temperature variation of the Rio Grande, the temperature range of 8.9 to 18.4 °C corresponds to recharge in the modern seasonal periods of mid-March to early June, and of mid-September to late November. Recharge to the Central zone occurs predominantly in spring when river discharge is high.

The coolest average recharge temperatures retrieved from paleo Rio Grande water samples were from the period 15–27 ka B.P., and warmest from the period 5–9 ka B.P.; however, because the standard deviations of the two groups overlap, it is only possible to conclude that the average temperature of Rio Grande water recharged to the MRGB has been nearly constant for the past 27 ka, and within about 1 °C of the modern mean annual temperature. This result seems to contradict the observed cooling of some 5 °C at higher altitudes along the basin margins during the LGM [*Phillips et al.*, 1986; *Stute et al.*, 1992, 1995].

One possible explanation of the apparent lack of paleoclimatic variation in average Rio Grande water temperatures over the past 27 ka may be in the timing of peak discharge of the Rio Grande, which probably was later during cold periods and earlier in warm climates. If, during the LGM, the mean annual temperature in the southwestern U.S. lowered approximately 5 °C relative to the modern mean annual temperature, the observed range of recharge temperatures of paleo Rio Grande waters (8.9–18.4 °C), representing the time of peak discharge in the Rio Grande, indicates that the season of peak discharge and peak infiltration of Rio Grande water to the aquifer system shifted approximately 30–60 days later into the summer, resulting in peak Rio Grande runoff from mountain snowmelt occurring in June and July, rather than April and May as is observed today. As a result, the paleo water temperatures of the Rio Grande during peak discharge, as recorded in the dissolved N_2 and Ar concentrations in groundwater infiltration from the river, would appear to be nearly constant through time.

Of the two scenarios discussed earlier to explain the historical variations in stable isotopic composition of Central zone groundwater, the evidence from the N_2-Ar recharge temperatures is consistent with the hypothesis of a seasonal shift in the timing of peak river discharge.

Although the average recharge temperature of paleo Rio Grande water has been nearly constant over time, there are small differences in average recharge temperatures that may have some significance, particularly during the past 5 ka. Since the mid-Holocene warm period (4–8 ka B.P.), there has been a small shift in the average temperature of Rio Grande water recharged to the MRGB, being about 1.5 °C cooler today relative to that of the mid-Holocene warm period. In the past 5 ka, the decrease of about 7 per mil in δ^2H of water recharged along the Eastern Mountain Front (Figure 5) (if the result of temperature changes only), indicates average cooling along the eastern basin margin of about 1.4 °C [*Straaten and Mook*, 1983]. However, further study is needed to determine if other processes, such as change in moisture source or shift in predominant season of recharge, could account for the decrease in δ^2H along the basin margin during the past 5 ka. More reliable indicators of recent climatic change can be found in the stalagmite record of *Polyak et al.* [2001], which indicates a cooler, wetter climate during the period 3,200 to 800 years, B.P., that changed to the present warmer and dryer climate about 800 years ago.

Stable isotopes and dissolved gases: Eastern Mountain Front and West-Central zones. Recharge temperatures of waters from the Eastern Mountain Front zone are compared with recharge temperatures of waters from the West-Central zone in Figure 8. The labels on the data points of Figure 8 give the corresponding value of δ^2H, in per mil, of water in the sample. Most of the samples with the lowest recharge temperatures from the West-Central zone also are depleted in ^2H, consistent with focused recharge at higher altitude. Most of the samples from the West-Central zone with warm recharge temperatures that were recharged during the last glacial period are enriched in ^2H relative to those with low recharge temperatures (Figure 8), consistent with diffuse recharge of precipitation falling at relatively low altitude.

From measurements of the stable isotopic composition of groundwater from springs and wells along the flanks of the Jemez Mountains, *Vuataz and Goff* [1986] found that δ^2H varies with altitude according to the relation, $\Delta\delta^2H/\Delta E$ = -2.2 per mil per 100 m altitude. This observed dependence of δ^2H on altitude can be derived from the temperature dependence of stable isotope fractionation and the lapse rate [*Plummer et al.*, 2004]. Using the relation of *Vuataz and Goff* [1986], the range in δ^2H values found for waters from the West-Central zone recharged during the last glacial period (δ^2H = –81 to –110 per mil) represents precipitation that fell over a range in altitude of approximately 1,200 m.

Waters from the Eastern Mountain Front zone vary less in their stable isotope composition than waters from the West-Central zone, presumably because recharge altitude varies less for waters from the Eastern Mountain Front zone than for waters from the West-Central zone. Most of the waters from the Eastern Mountain Front zone have δ^2H values of about –71 to –87 per mil (Figure 8), which could represent precipitation that fell over a range of approximately 700 m in altitude. Yet both the West-Central and Eastern Mountain Front zones contain water recharged either as focused or diffuse infiltration, resulting in a wide range of recharge temperatures recorded in dissolved N_2 and Ar concentrations.

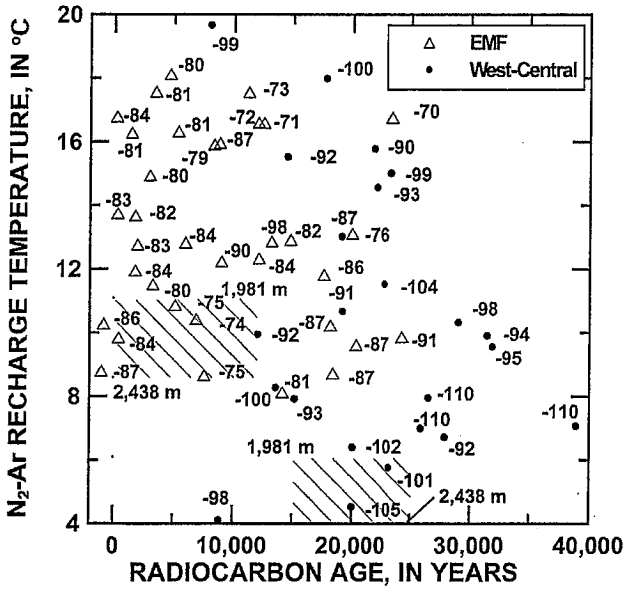

Figure 8. Comparison of N_2-Ar recharge temperatures for waters from the Eastern Mountain Front (EMF) and West-Central zone as a function of radiocarbon age. The labels are values of δ^2H in per mil for the water sample. An uncertainty of ± 450 m in recharge altitude results in an uncertainty of ± 2 °C in recharge temperature. The shaded patterns show the modern and LGM estimated mean annual temperatures for recharge at 1,981 and 2,438 m. Most samples have recharge temperatures that are warmer than the estimated mean annual temperature.

The examples above demonstrate some of the difficulties that can arise in attempts to interpret paleo-recharge conditions from dissolved gas and stable isotope data, particularly in mountainous arid regions where there can be large variations in recharge altitude, and recharge temperatures can be biased warm if infiltration is through a deep unsaturated zone.

ESTIMATION OF MODERN AND PALEORECHARGE

A groundwater-flow model developed for the MRGB with MODFLOW [*McDonald and Harbaugh,* 1988] was used to estimate recharge to the basin. Travel times to observation wells were calculated using MODPATH [*Pollock,* 1994]. The MODFLOW and MODPATH representations of the basin were calibrated using UCODE [*Poeter and Hill,* 1998]. The model domain was divided into a rectilinear grid comprised of 156 rows and 80 columns of equally spaced 1-km size cells (Plate 5). The eastern and western model boundaries mostly are coincident with faults that either act as barriers to horizontal groundwater movement or separate areas with different thickness of permeable sediment [*Kernodle et al.,* 1995]. The vertical extent of the aquifer system is represented by nine model layers. The upper seven layers range in thickness from 6 to 300 m, whereas layers 8 and 9 are of variable thickness and represent the aquifer system from the bottom of model layer seven down to the base of the Santa Fe Group sediments at 2,400 m below sea level at the deepest point.

River-cell boundaries were implemented over the width of the inner valley of the MRGB to represent the interaction of the Rio Grande with the aquifer system. Likewise, river-cell boundaries were implemented along the Jemez River and Rio Puerco to represent the groundwater/surface-water interaction along those waterways. River cells were applied across the entire floodplains because rivers migrate across their floodplains over thousand of years, and the objective was to simulate this long-term average condition. Mountain-front recharge and arroyo infiltration were simulated using recharge cells. The recharge was divided into segments along the eastern and southern mountain fronts and arroyos (Plate 5). Underflow along the basin boundaries was simulated using the well package of MODFLOW. Several underflow segments were specified, extending the length of the northern and western model boundaries. The hydraulic conductivity zones for the basin were based on the three-dimensional geologic model of *Cole* [2001]. A total of 18 hydraulic conductivity zones were defined within the groundwater-flow model [*Sanford et al.,* 2004]. Vertical conductances in the groundwater-flow model were divided into twelve zones—the associated parameters were represented as values of vertical anisotropy. Two fault zones, representative of the Cat Mesa fault zone in the southwestern part of the basin and the Sandia Fault zone along the eastern mountain front at Albuquerque (Figure 1), were added to the groundwater-flow model as discrete (low) hydraulic conductivity zones.

Porosity for the unconsolidated sediment of the MRGB was estimated from field measurements. *Stone et al.* [1998] reported total porosity values between 30 and 40 percent from a 457 m core of the Santa Fe Group. *Haneberg* [1995] reported porosity values derived from geophysical logs that range from about 40 percent at the land surface to about 30 percent at 300 m depth. Based on this information, porosities were assigned by layers beginning with 36 percent for model layer 1 and decreasing 2 percent per layer down to 20 percent for layer 9.

The investigation incorporated hydrochemical tracer data into the calibration of the groundwater-flow model. Groundwater ages obtained from ^{14}C activities were one set of these data. Simulated ages were obtained by using MODPATH to track the line of travel of a parcel of water from the

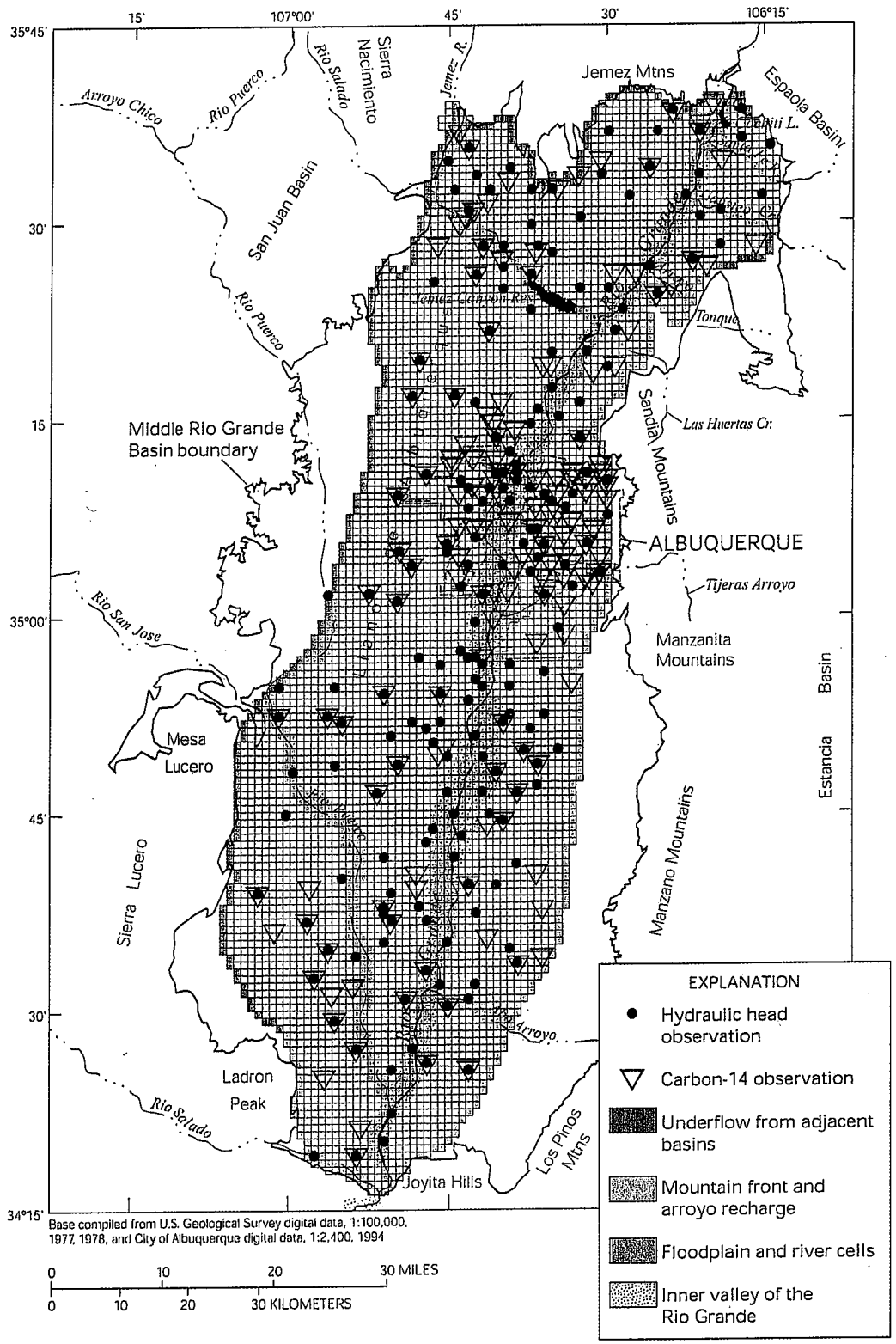

Plate 5. Finite-difference grid, locations and types of boundary conditions, and locations of hydraulic head and ^{14}C observations for the groundwater model.

observation well backward to its recharge location. Time-of-travel was integrated backward along path lines to obtain simulated groundwater ages. Hydrodynamic dispersion in these calculations was neglected, as the effect of dispersion on the concentrations from a nearly invariant source over a 100 km basin would be negligible for values of longitudinal dispersivity less than 1 km [*Phillips et al.*, 1989; *Johnson and DePaolo*, 1996].

Another source of tracer information that was used for model calibration was the delineation of the hydrochemical zones (Figure 4), representing different water sources. MODPATH was used to simulate the locations of the boundaries between hydrochemical zones, which were compared to the observed locations (Figure 4).

The relation between simulated groundwater age and simulated ^{14}C activity is based on radioactive decay, according to the equation:

$$pmC = A_0/(\exp(\text{time} \times \ln(2)/5730)), \quad (1)$$

where A_0 is the ^{14}C activity at the recharge location, "time" is the simulated travel time from MODPATH, and 5,730 is the half-life of ^{14}C, in years. The calculated mixing effects and effects of geochemical reactions [from NETPATH, *Plummer et al.*, 2004], and the transient atmospheric effects (radiocarbon calibration) were incorporated into a value of A_0 assigned to each individual water sample. In MODPATH, one parcel of water was tracked backward for each 30 m of observation well screen. All of the simulated travel times for a well first were converted to simulated ^{14}C activity using eq. 1, then the average activity was calculated for the entire well. In this manner, a mixing effect was added to the final simulated ^{14}C age for long-screened wells. Backward tracking in MODPATH traces the path lines to the location where that water would have entered the model of the basin. At underflow boundaries, this location does not coincide with a recharge location for the water where the ^{14}C activity would obtain its initial value. For these boundaries, an initial age was assigned for the water as it enters the basin. This initial age was added to the path-line age calculated by MODPATH. These initial ages were treated as model parameters that were estimated during the inverse procedure.

Calibration of the Groundwater-Flow Model

The groundwater model was calibrated using a combination of a nonlinear least-squares regression method as it is implemented in the computer code UCODE [*Poeter and Hill*, 1998], and manual adjustment of individual parameters. For this study MODFLOW and MODPATH were called by UCODE during each regression iteration. Although UCODE was run to reduce the model error, the discrete nature of the particle tracking prohibited the nonlinear regression method from obtaining the optimum fit. After the UCODE regression, individual parameters were adjusted manually and sequentially to obtain the best fit. Accuracy of the sensitivity calculations was limited by the discrete nature of the path-line calculations. UCODE also was used during manual parameter adjustment to run multiple simulations varying only one parameter at a time over a finite range of values. A range of values for each parameter was examined in this way individually, adjusting the value of each one to the point of minimum global error.

Multiple data types were used in this study to calibrate the groundwater-flow model. Hydraulic heads, ^{14}C activity, and the locations of the hydrochemical zones were all used as observations in the objective function. These values were all given weights in accordance with their perceived or estimated accuracy. A total of 200 hydraulic heads, 200 ^{14}C activity measurements, and the fraction of river water in 9 geochemical target regions were used as observations, making a grand total of 409 observations [*Sanford et al.*, 2004]. Head and ^{14}C data locations are shown in Plate 5.

The groundwater model first was set up to simulate steady-state groundwater flow prior to the development of groundwater as a resource within the basin. The head data were compiled by *Bexfield and Anderholm* [2000] from many sources (Figure 2). The expected measurement errors for the hydraulic heads were estimated to be between 0.3 m for recent surveyed monitoring wells and 3 m or more for domestic wells, where the measuring-point altitude was estimated from a topographic map. These estimated measurement errors were used to assign weights to the head observations. Weights for the ^{14}C activities were more difficult to determine on a well-by-well basis because it was difficult to assess how the influx of water to a well varied vertically within the well screen. A simple weighting scheme was adopted where an uncertainty of 1 and 5 pmC was assigned to short- and long-screened wells, respectively.

In addition to water levels and ^{14}C activity data, the location and extent of certain of the hydrochemical zones were used as observations. Earlier idealized simulations of the basin indicated that the volume of Rio Grande and Rio Puerco water present in the aquifer system would depend upon the recharge and hydraulic conductivity of model parameters [*Sanford et al.*, 1998]. The less the recharge along the margins of the basin, or the higher the hydraulic conductivity of the aquifer, the broader is the regional extent of the recharged river water that is present adjacent to the

river. Hydrochemical zones were delineated clearly for Rio Grande water and Rio Puerco water, and, thus, could be used as observations. As the exact positions of the boundaries between the hydrochemical zones were a function of the recharge and hydraulic conductivity parameters in the groundwater model, those boundary positions were used as observations in the model calibration.

Nine geochemical target regions were used as observations [*Sanford et al.*, 2004]. The observation value was the percentage of river water observed to be in a given target-region based on the hydrochemical zone delineation. To simulate this, thousands of particles were generated for each target region in an array pattern using MODPATH and tracked backward to the source. The number of paths originating from the river was then divided by the total number of paths for that target region. The large number of particles allowed this simulated percentage to vary by finite and appreciable amounts when each parameter was perturbed by only a few percent.

Sensitivities were calculated for each of the parameters from both the MODFLOW and MODPATH model simulations. Based partially on the magnitude of the sensitivity and partially on the availability of prior information, some parameters were assigned values and others were estimated using the nonlinear regression. The parameters with the highest sensitivities were the hydraulic conductivities in the southern and east-central areas of the basin, the anisotropy of the Rio Grande alluvium near Albuquerque, recharge values for the southern Sandia Mountain front, and underflow from the northern and northwestern boundaries. Based on low sensitivities, values were assigned to the vertical leakance of the northern and southern sections of the Rio Grande, and to the hydraulic conductivity of the Cat Mesa fault zone.

Model Results

The hydraulic heads from the final simulation (Figure 9) matched relatively well with the observed heads. The final model configuration reproduced the groundwater trough that extends north to south through the west-central part of the basin, although not as far north as some of the measured water levels indicate (Figure 2). Earlier models [e.g. *Kernodle et al.*, 1995] did not manage to reproduce this feature. Attempts also were made by *Tiedeman et al.* [1998] to investigate different conceptual models of what was creating the trough, including a high permeability zone or a north-south trending fault. Earlier prototype models [*Sanford et al.*, 1998], however, demonstrated that by lowering the basin boundary recharge in the model, the aquifer system changed from one dominated by the movement of water from the boundaries toward the Rio Grande to one dominated by water leaking from and back into the Rio Grande. The latter conceptual system results in heads to the west of the Rio Grande that are lower than the river, and is consistent with the presence of the trough and the relatively low recharge values estimated with the model. The final model configuration also reproduces the losing section of the Rio Grande that occurs just north of Albuquerque (Figure 9).

From the contours (Figure 9), one can see that groundwater moves away from the Rio Grande both to the west toward the trough, and to the south beneath the city of Albuquerque, as also is shown by the predevelopment water-table map (Figure 2). This zone of Rio Grande water beneath the city also is corroborated by the hydrochemical zone delineation (Figure 4). The Rio Grande water (Central hydrochemical zone) does not extend fully westward into the trough, indicating that the trough is a more transient and recent feature than the hydrochemical zones, appearing with the decrease in recharge that followed the LGM. Rio Grande water has not yet reached its fullest extent into the trough region.

Simulated ages were plotted by placing a 10-by-10 grid of particles in every model cell, and tracking the path lines backward to the source location. All of these ages were then plotted as a function of their starting locations to produce the images in Plate 6. Young water (< 3,000 years), represented by the dark blue areas, is present near the mountain fronts where recharge occurs at the land surface, and along the Rio Grande and Rio Puerco near where the rivers are losing water to the aquifer system. A cross section of the simulated ages reveals a general pattern of increasing simulated age with depth, but the heterogeneity of the system in some places creates local inversions where old water is simulated above younger water moving through a more permeable zone. The geochemical zones also were simulated using MODPATH using source-area delineation of path lines. The zones are delineated and labeled in Plate 6.

Values for hydraulic conductivities were calibrated to values mostly between $3x10^{-6}$ and $3x10^{-5}$ ms^{-1}, and were similar to estimates from previous models [*Kernodle et al.*, 1995; *Tiedeman et al.*, 1998; *McAda and Barroll*, 2002] and prior field measurements concerning the basin fill material [*Thorn et al.*, 1993]. The anisotropy (K_v/K_h) was calibrated for 12 individual zones within the basin, and the calibrated values all ranged between $1x10^{-4}$ and $1x10^{-2}$. These values are consistent with what might be expected for a layered aquifer system where the individual layers are isotropic and have hydraulic conductivity values that vary by 2 to 4 orders of magnitude.

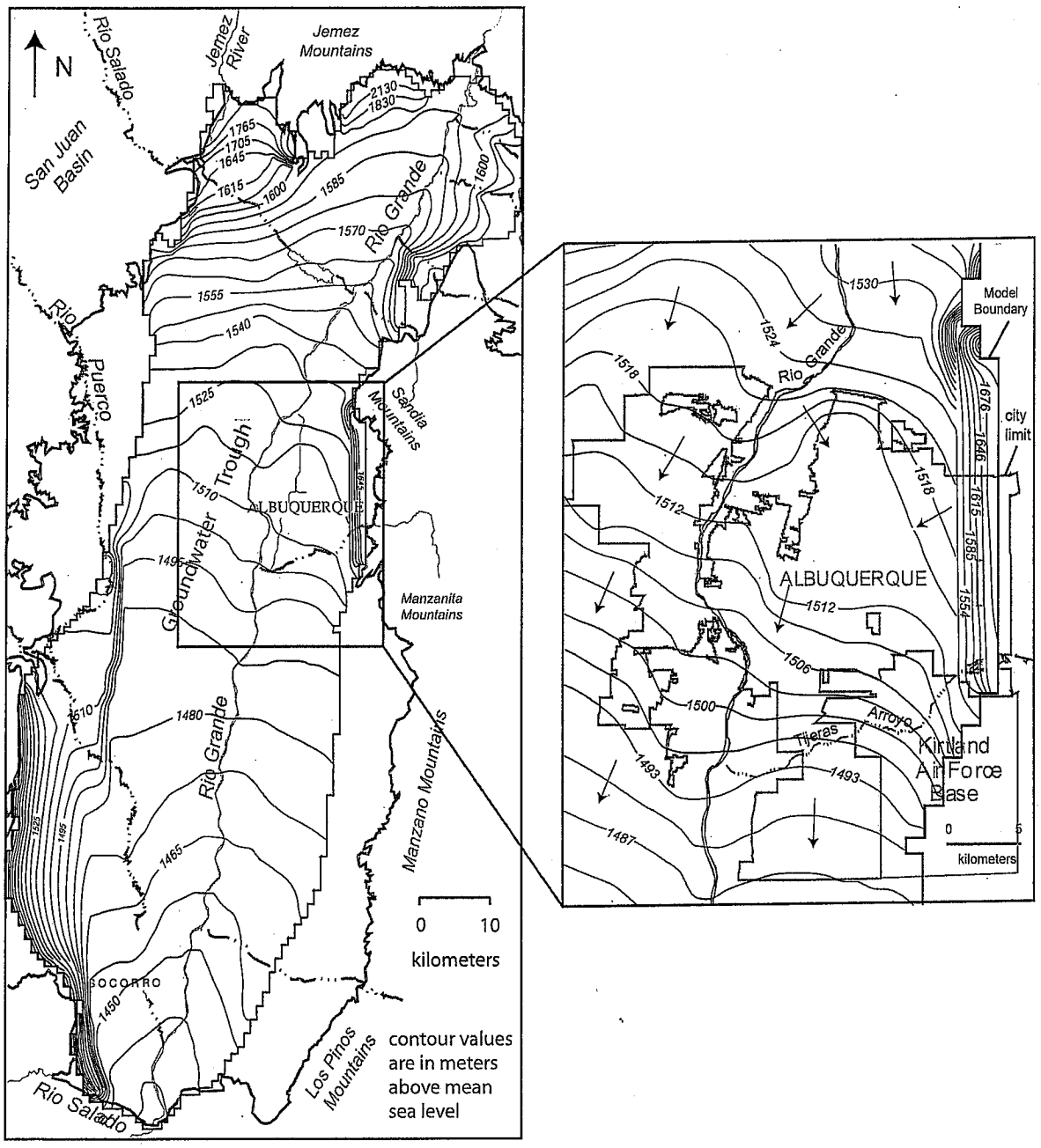

Figure 9. Simulated hydraulic head in layer 2 of the groundwater model. Arrows indicate generalized direction of groundwater flow.

Recharge was not specified directly for the Rio Puerco and the Jemez River in the model, but was calculated through their riverbed conductance values. The calculated recharge rates were 0.14 m^3s^{-1} for the Rio Puerco and 0.01 m^3s^{-1} for the Jemez River (Table 4). The recharge for the Rio Puerco was similar to values used in earlier models, but the Jemez River recharge value was much lower. Recharge from the eastern mountain front was estimated to be 0.33 m^3s^{-1}, with 0.04 m^3s^{-1} of additional recharge from Abo Arroyo. These numbers are appreciably lower than previous estimates that were based on rainfall-runoff equations [*Kernodle et al.*, 1995], but are similar to recent estimates of recharge of 0.35 and 0.05 m^3s^{-1} along the eastern mountain front and Abo Arroyo and vicinity, respectively, made from

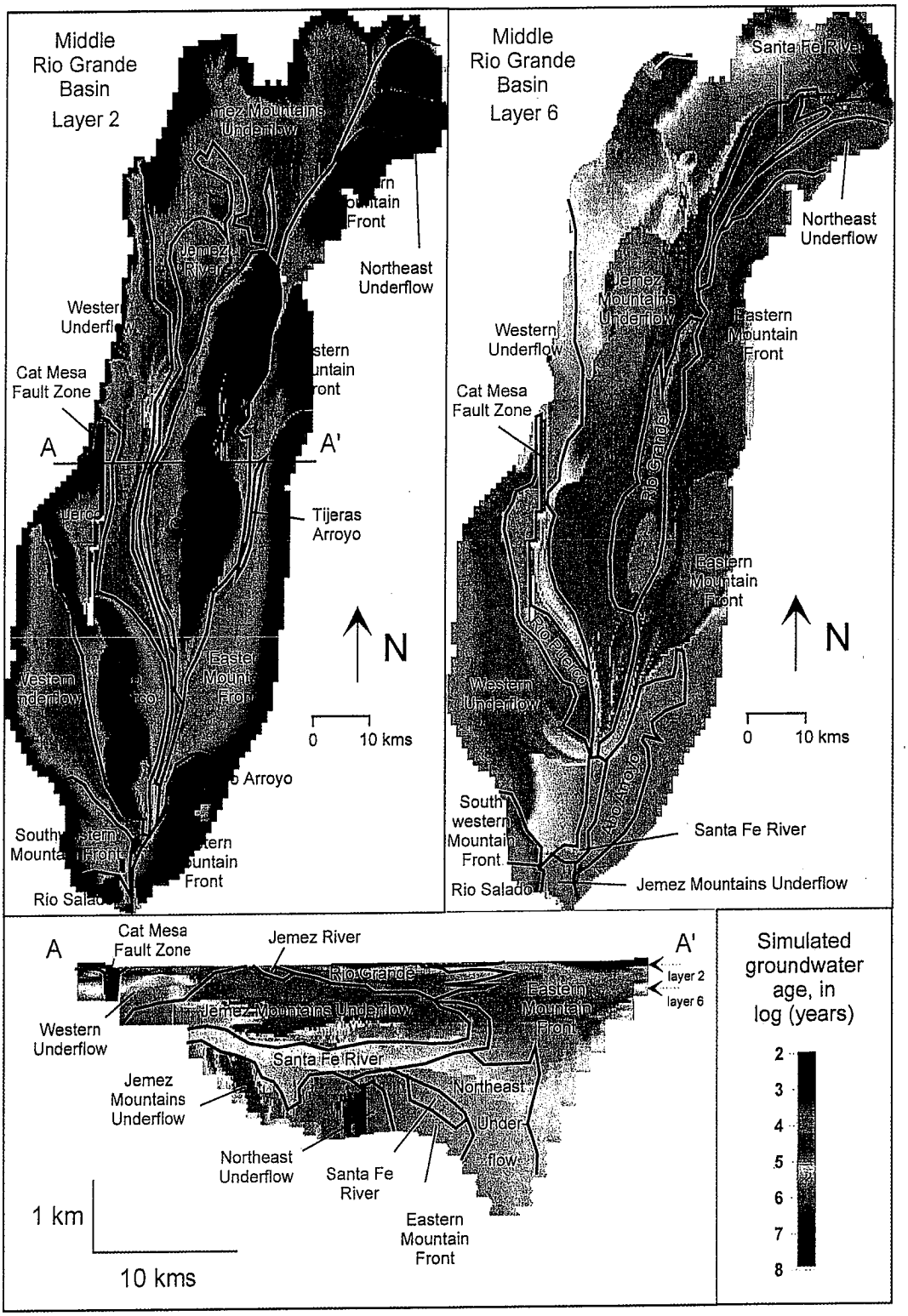

Plate 6. Simulated groundwater ages from the groundwater-flow model at relatively shallow depths (50–100 m, model layer 2) and deeper depths (300–500 m, model layer 6). Simulated hydrochemical zones (source areas) are delineated by black lines and labeled.

Table 4. Estimates of recharge to the Middle Rio Grande Basin (m^3/sec) from recent studies

Region	Kernodle et al. (1995)	Tiedeman et al. (1998)	Anderholm (2001)	McAda & Barroll (2002)	This Study
Jemez Mountains	0.56	0.27	N/A	0.58	0.08
WB[b]	0.18	0.18	N/A	0.07	0.06
SWB[b]	0.30	0.09	N/A	0.03	0.17
San Juan Basin	0.05	0.05	N/A	0.04	0.27
H-E Basin[b]	0.21	0.49	N/A	0.55	0.03
Northeast rivers	0.32	0.30	N/A	0.21	0.18
Tijeras Arroyo	0.41	0.41	0.07	0.03	0.00
Abo Arroyo	0.62	0.60	0.05	0.05	0.04
Rio Puerco	0.23	0.12	N/A	0.04	0.14
Jemez River	0.48	0.48	N/A	0.59	0.01
Rio Grande[a]	0.00	0.00	N/A	N/A	0.78
Rio Salado	0.28	0.28	N/A	0.08	0.06
Sandia Mtn front	0.74	0.41	0.16	0.21	0.16
SEMF[b]	1.06	1.16	0.19	0.16	0.17
Total	5.45	4.86	N/A	2.63	2.14

[a]This number represents loss from the inner valley to the Santa Fe Group aquifer system. The early models calculated significant loss of water from the Rio Grande, but it is clear from their simulated head contours that this was all immediately lost to ET in the inner valley—none of it reached the Santa Fe Group aquifer system outside the inner valley. McAda and Barroll (2002) also calculated an appreciable loss from the Rio Grande, but their model results did not indicate whether any of that loss left the inner valley.

[b]WB, Western Boundary; SWB, Southwest Boundary; H-E Basin, Hagan/Espanola Basin; SEMF, Southeast Mountain Front

a field study of chloride mass-balance [*Anderholm*, 2001]. *McAda and Barroll* [2002] recently created a groundwater-flow model of the basin partially incorporating preliminary results from this study. They used a combination of some higher recharge values used in the earlier studies, and lower values estimated by *Anderholm* [2001], and in this study. Total recharge to the basin in this study was estimated from the model to be 2.14 m^3s^{-1}, with 0.78 m^3s^{-1} of the total leaking from the Rio Grande. The basin-margin recharge estimated from the model described in this report, 1.37 m^3s^{-1}, is one-fourth of the 5.45 m^3s^{-1} estimate used in the 1995 Kernodle model and one-half of that used by *McAda and Barroll* [2002]. Overall, the lower recharge values are consistent with the presence of the groundwater trough and zone of Rio Grande water in the central basin. *McAda and Barroll* [2002] partially reproduced these features by adding N-S trending fault barriers in the center of the basin.

A transient groundwater-flow simulation was performed to investigate the effect of time-varying recharge rates over the past tens of thousands of years on simulated ^{14}C activities. A 30,000-year simulation first was run with six 5,000-year time steps [*Sanford et al.*, 2001], and most recently with an updated model using twelve 2,500-year time steps. During each of the time steps, all recharge and underflow boundary cells were multiplied by a single coefficient. These coefficients, or multipliers, all were given an initial value of 1.0 to reproduce the conditions in the steady-state simulation. The multiplier for each time step was then adjusted until an optimum fit was obtained between the measured and simulated observations. The nonlinear regression routine in UCODE initially was used to reduce the total sum of the squared errors, but eventually the individual recharge multipliers were adjusted manually to obtain the "best-fit" multiplier values.

Results from the transient simulation indicate that recharge was greater before 15,000 years ago (Figure 10) than today. The optimal values for the recharge multipliers are greater than 10 for the period between 20 ka and 25 ka B.P. The earlier simulation using unadjusted ^{14}C activities and 5,000-year time steps suggested an increase in recharge during the LGM of 5-6 times. Evidence for a wetter climate during this period is present in the Estancia Basin, just east of the Sandia Mountains, in the form of playa lake deposits [*Bachhuber*, 1992; *Allen and Anderson*, 2000]. The more recent simulation with 2,500-year time steps indicated that recharge during the LGM was over 10 times greater than today. Although precipitation may have increased by a factor of approximately 2.5 during the LGM relative to today [*Thompson et al.*, 1999], a small percentage increase in rainfall in arid regions can easily lead to a much larger percentage increase in recharge. In both transient simulations the paleorecharge rates were accompanied by high degrees of uncertainty. Underflows 10 times modern rates also would require hydraulic gradients 10 times greater, and this rate is highly unlikely, if not physically impossible in some regions. Also, vertical transverse dispersivity likely contributes additional ^{14}C to some older waters of the basin, leading to ages that are younger than advective travel times, and, in turn, higher paleorecharge rates. The highest values of paleorecharge predicted should, therefore, be seen as maximum rates, and likely greater than the actual rates. Both sets of results also consistently point to an amount of recharge just before or at the beginning of the Holocene that was lower than modern values (Figure 10).

CONCLUSIONS

Chemical and isotopic data for groundwater from throughout the Middle Rio Grande Basin, New Mexico, were used to identify 12 sources of recharge to the basin and

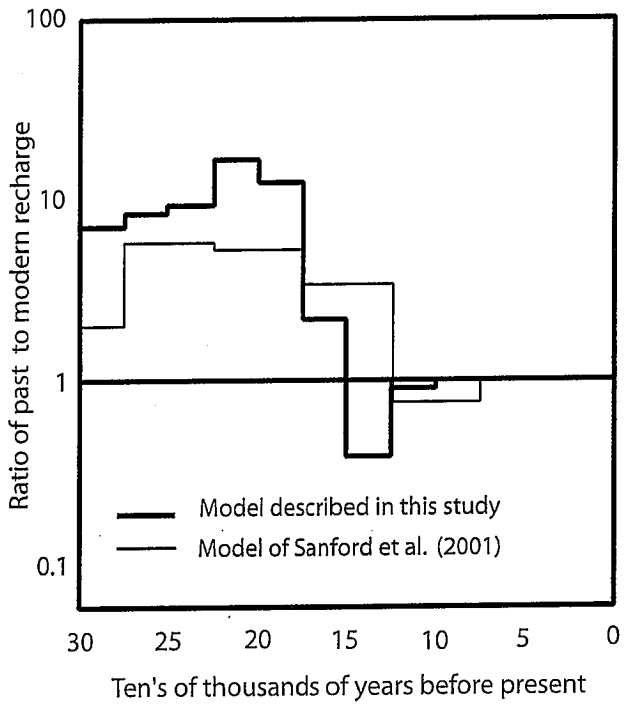

Figure 10. Paleorecharge estimates from groundwater models.

a zone of groundwater discharge. Predominant sources of water to the basin include (1) mountain-front recharge along the north, east and southwestern margins of the basin (median age 5-9 ka); (2) seepage from the Rio Grande and Rio Puerco (median age 4-8 ka), and, to a lesser extent, Abo and Tijeras Arroyo (median age 3–9 ka); (3) inflow of saline water along the southwest basin margin (median age 20.4 ka); and (4) inflow along the northern basin margin that probably represents recharge from the Jemez Mountains during the last glacial period (median age 19.9 ka). This latter source is at the water table through the west-central part of the MRGB, beneath recharge from the Rio Grande at Albuquerque and beneath younger northern mountain-front recharge along the northern margin of the basin.

Geochemical mass-balance calculations show that water-rock reactions were minimal in the primarily siliciclastic basin-fill sediment, leading to well-defined radiocarbon ages that range from modern to more than 30 ka B.P. Deuterium contents for the various sources of groundwater recharged to the basin are relatively distinctive, and were of considerable use in tracing groundwater flow. Chlorofluorocarbon and tritium data showed that recharge has occurred within the past 30–50 years in parts of the inner valley of the Rio Grande and near mountain fronts along the basin margin.

During the past 5 ka, δ^2H of water from the Central hydrochemical zone (Rio Grande origin) increased by nearly 6 per mil from a minimum near –98 per mil; and δ^2H of moisture recharged along the Eastern Mountain front became more depleted in ^2H, by about 7 per mil. The δ^2H isotopic composition of water recharged from the Rio Grande to the Central zone was a minimum at approximately 5 ka B.P., a maximum at about 15 ka B.P., and again relatively depleted at about 22 ka B.P. Dissolved N_2 and Ar concentrations in paleowater recharged from the Rio Grande indicate that the average temperature of Rio Grande water recharged to the MRGB has been nearly constant for the past 27 ka, and within about 1 °C of the modern mean annual temperature. These observations appear consistent with the hypotheses of (1) a seasonal shift in the timing of peak river discharge, occurring later during cold periods and earlier when the climate is warmer, and (2) changes in amounts of low-altitude precipitation occurring along the basin margins. The shift in stable isotopic composition of recharge along the eastern mountain front indicates an average cooling of about 1.4 °C during the past 5 ka. The dissolved N_2-Ar data show that recharge temperatures can be biased warm, if infiltration is through deep unsaturated zones.

The hydrochemical tracer data (^{14}C and delineation of hydrochemical zone boundaries) were incorporated into the calibration of a groundwater-flow model that then was used to estimate recharge to the MRGB. Recharge rates determined from the groundwater model were appreciably lower than previous estimates based on a rainfall-runoff model, but in agreement with low recharge estimates determined from the chloride mass-balance method. The model simulation indicates that the relatively low recharge rates may result in the formation of a groundwater trough that extends through much of the center of the basin and account for the presence of a substantial quantity of Rio Grande water in the Santa Fe Group aquifer system. Earlier models of the basin had difficulty reproducing these features without use of hydrochemical data to constrain the rates and distribution of recharge. Results from a 30,000-year transient simulation suggest that recharge at the LGM may have been ten times the modern rate, but that recharge following the LGM was about 60 percent of the modern rate.

Acknowledgments. The authors thank the numerous individual landowners who provided access to their wells. We thank the Governors and staffs of the Pueblos of Cochiti, Isleta, Jemez, Sandia, San Felipe, Santa Ana, Santo Domingo, and Zia, New Mexico for permitting us to sample wells, and assisting in locating both wells and records of well construction. The authors also thank Bill White with the Bureau of Indian Affairs for his assistance in contacting the Pueblos and his advice about the most appropriate wells for sampling. Water samples from many of the windmills on Pueblo lands could not have been obtained without the generous

assistance of John Sanchez and the windmill crew of the Southern Pueblos Agency.

Individuals from the U.S. Forest Service, the Bureau of Land Management, the U.S. Fish and Wildlife Service, Kirtland Air Force Base, Sandia National Laboratories, the New Mexico Office of the State Engineer, the New Mexico Environment Department, the University of New Mexico, the city of Albuquerque, the city of Belen, and the Town of Los Lunas provided access to wells and assisted in locating the most appropriate wells for sampling. We thank Doug Earp and others with the city of Albuquerque Environment Department for their assistance. The cooperation of Rio Rancho Utilities, Rio Grande Utilities, Sandia Peak Utility Company, National Utilities, New Mexico Utilities, DRESCO, Intel, AT&T, King Brothers Ranch, and the Huning Ltd. Partnership in providing access to wells is gratefully acknowledged.

We thank our colleagues with the USGS, Jerry Casile, Mike Doughten, Julian Wayland, Peggy Widman, Andrew Stack, Anne Burton, Brian C. Norton, David Jones, Ami Mitchell, Daniel Webster, Tyler Coplen, Kinga Revesz, Robert L. Michel, Fred Gebhardt, R.K. DeWees, Jim Bartolino, Joe Sterling, Carolina Trevizo, and Lori Shue for assistance in field sampling, laboratory analysis, assistance in locating wells, data processing, drafting of illustrations, and manuscript preparation.

Finally, the authors would like to thank Doug McAda, Mark Hudson, and Scott Minor of the USGS, Fred Phillips of New Mexico Tech, and John Hawley and Sean Connell of the New Mexico Bureau of Geology and Mineral Resources (NMBGMR) who shared their knowledge and advice about the hydrology and geology of the basin. An earlier version of this report was improved appreciably by the technical reviews of Jim Bartolino and Don Thorstenson. We thank James Hogan and Tom Maddock for their technical reviews of the manuscript.

REFERENCES

Allen, B. D., and R. Y. Anderson, A continuous, high-resolution record of late Pleistocene climate variability from the Estancia basin, New Mexico, *Geol. Soc. Am. Bull., 112*, 1444-1458, 2000.

Anderholm, S. K., Ground-water geochemistry of the Albuquerque-Belen Basin, Central New Mexico, *U.S. Geol. Surv. Water-Resour. Invest. Rep. 86-4094*, 110 pp., 1988.

Anderholm, S. K., Mountain-front recharge along the east side of the Albuquerque Basin, Central New Mexico (revised), *U.S. Geol. Surv. Water-Resour. Invest. Rep. 00-4010*, 36 pp., 2001.

Bachhuber, F. W., A pre-late Wisconsin paleolimnologic record from the Estancia Valley, central New Mexico, in *The Last Interglacial-Glacial Transition in North America*, edited by P. U. Clark and P. D. Lea, pp. 289-307, *Geol. Soc. Am. Spec. Pap. 270*, 1992.

Bartolino, J. R., and J. C. Cole, Ground-water resources of the Middle Rio Grande Basin, New Mexico, *U.S. Geol. Surv. Circ. 1222*, 132 pp., 2002.

Benson, L. V., D. R. Currey, R. I. Dorn, K. R. Lajoie, C. G. Oviatt, S. W. Robinson, G. I. Smith, and S. Stine, Chronology of expansion and contraction of four Great Basin lake systems during the past 35,000 years, *Palaeogeogr., Palaeoclimat., Palaeoecol., 78*, 241-286, 1990.

Bexfield, L. M., and S. K. Anderholm, Predevelopment water-level map of the Santa Fe Group aquifer system in the Middle Rio Grande Basin between Cochiti Lake and San Acacia, New Mexico, *U.S. Geol. Surv. Water-Resour. Invest. Rep. 00-4249*, 1 sheet, 2000.

Bexfield, L. M., and S. K. Anderholm, Estimated water-level declines in the Santa Fe Group aquifer system in the Albuquerque area, central New Mexico, predevelopment to 2002, *U.S. Geol. Surv. Water-Resour. Invest. Rep. 02-4233*, 1 sheet, 2002.

Bjorklund, L. J., and B. W. Maxwell, Availability of groundwater in the Albuquerque area, Bernalillo and Sandoval Counties, New Mexico, *New Mexico State Engineer Tech. Rep. 21*, 117 pp., 1961.

Busenberg, E., E. P. Weeks, L. N. Plummer, and R. C. Bartholomay, Age dating groundwater by use of chlorofluorocarbons (CCl_3F and CCl_2F_2), and distribution of chlorofluorocarbons in the unsaturated zone, Snake River Plain aquifer, Idaho National Engineering Laboratory, Idaho, *U.S. Geol. Surv. Water-Resour. Invest. Rep. 93-4054*, 47 pp., 1993.

Cayan, D. R., S. A. Kammerdiener, M. D. Dettinger, J. M. Caprio, and D. H. Peterson, Changes in the onset of spring in the western United States, *Am. Meteor. Soc. Bull., 82*, 399-415, 2001.

Cole, J. C., 3-D geologic modeling of regional hydrostratigraphic units in the Albuquerque segment of the Rio Grande rift, in *U. S. Geological Survey Middle Rio Grande Basin Study—Proceedings of the Fourth Annual Workshop, Albuquerque, New Mexico, February 15-16, 2000, U. S. Geol. Surv. Open-File Rep. 00-488*, edited by J.C. Cole, pp. 26-28, 2001.

Ellis, S. R., G. W. Levings, L.F. Carter, S.F. Richey, and M.J. Radell, Rio Grande Valley, Colorado, New Mexico, and Texas, *Am. Water Resour. Assoc., Water Resour. Bull., 29*, 617-646, 1993.

Gee, G. W., and D. Hillel, Ground-water recharge in arid regions: Review and critique of estimation methods, *Hydrol. Processes, 2*, 255-266, 1988.

Grissino-Mayer, H., Tree-ring reconstructions of climate and fire history at El Malpais National Monument, New Mexico, Ph.D. thesis, The University of Arizona, Tucson, 1995.

Grissino-Mayer, H., A 2129-year reconstruction of precipitation for northwestern New Mexico, U.S.A., in *Tree Rings, Environment and Humanity*, edited by J. S. Dean, D. M. Meko, and T. W. Swetnam, pp. 191-204, *Radiocarbon*, Tucson, 1996.

Haneberg, W. C., Depth-porosity relationships and virgin specific storage estimates for the upper Santa Fe Group aquifer system, central Albuquerque Basin, New Mexico, *New Mexico Geol., 17*, 62-71, 1995.

Hawley, J. W., and C. S. Haase, Hydrogeologic framework of the northern Albuquerque Basin, *New Mexico Bur. Mines and Mineral Resour., Open-File Report 387*, variously paged, Socorro, 1992.

Heaton, T. H. E., and J. C. Vogel, "Excess air" in groundwater, *J. Hydrol, 50*, 201-216, 1981.

Heaton, T. H. E., A. S. Talma, and J. C. Vogel, Origin and history of nitrate in confined groundwater in the Western Kalahari, *J. Hydrol., 62,* 243-262, 1983.

Johnson, T. M., and D. J. DePaolo, Reaction-transport models for radiocarbon in groundwater: The effects of longitudinal dispersion and the use of Sr isotope ratios to correct for water-rock interaction, *Water Resour. Res., 32*, 2203-2212, 1996.

Kernodle, J. M., Simulation of ground-water flow in the Albuquerque Basin, central New Mexico, 1901-95, with projections to 2020, *U.S. Geol. Surv. Open-File Rep. 96-0209*, 54 pp., 1998.

Kernodle, J. M., D. P. McAda, and C. R. Thorn, Simulation of ground-water flow in the Albuquerque Basin, central New Mexico, 1901-1994, with projections to 2020, *U.S. Geol. Surv. Water-Resour. Invest. Rep. 94-4251*, 114 pp., 1995.

Logan, L. M., Geochemistry of the Albuquerque municipal area, Albuquerque, New Mexico, MS thesis, New Mexico Inst. Mining and Tech., 282 pp., Socorro, 1990.

McAda, D. P., and P. Barroll, Simulation of ground-water flow in the Middle Rio Grande Basin between Cochiti and San Acacia, New Mexico, *U.S. Geol. Surv. Water-Resour. Invest. Rep. 02-4200*, 81pp., 2002.

McDonald, M. G., and A. W. Harbaugh, A modular three-dimensional finite-difference ground-water flow model, *U. S. Geol. Surv. Tech. Water-Resour. Invest., bk 6, chap. A1,* variously paged, 1988.

Meyer, H. W., Lapse rates and other variables applied to estimating paleoaltitudes from fossil floras, *Palaeogeogr. Palaeoclimat., Palaeoecol., 99*, 71-99, 1992.

Moore, D., Precipitation chemistry data on the Sevilleta National Wildlife Refuge, 1989-1995: Sevilleta LTER Database, accessed March 2, 1999, at http://sevilleta.unm.edu/research/local/nutrient/precipitation/#data, 1999.

Oviatt, C. G., D.R. Currey, and D. Sack, Radiocarbon chronology of Lake Bonneville, Eastern Great Basin, USA, *Palaeogeogr., Palaeoclimat., Palaeoecol., 99*, 225-241, 1992.

Phillips, F. M., L. A. Peeters, M. K. Tansey, and S. N. Davis, Paleoclimatic inferences from an isotopic investigation of groundwater in the San Juan Basin, New Mexico, *Quatern. Res., 26,* 179-193, 1986.

Phillips, F. M., M. K. Tansey, and L. A, Peeters, An isotopic investigation of groundwater in the central San Juan Basin, New Mexico: Carbon 14 dating as a basis for numerical flow modeling, *Water Resour. Res., 25*, 2259-2273, 1989.

Phillips, F. M., A. R. Campbell, C. Kruger, P. Johnson, R. Roberts, and E. Keyes, A reconstruction of the response of the water balance in western United States lake basins to climatic change, *New Mexico Water Resour. Res. Inst. Rep. 269*, 167 pp., 1992.

Plummer, L. N., E. C. Prestemon, and D. L. Parkhurst, An Interactive Code (NETPATH) for Modeling NET Geochemical Reactions Along a Flow PATH. Version 2.0, *U.S. Geol. Surv. Water-Resour. Invest. Rep. 94-4169*, 130 pp., 1994.

Plummer, L. N., L. M. Bexfield, S. K. Anderholm, W. E. Sanford, and E. Busenberg, E., Geochemical characterization of groundwater flow in parts of the Santa Fe Group aquifer system, Middle Rio Grande Basin, New Mexico, in *U.S. Geological Survey Middle Rio Grande Basin Study—Proceedings of the Fourth Annual Workshop, Albuquerque, New Mexico, February 15-16, 2000,* edited by J. C. Cole, pp. 7-10, *U.S. Geol. Surv. Open-File Rep. 00-488*, 2001.

Plummer, L. N., L. M. Bexfield, S. K. Anderholm, W. E. Sanford, and E. Busenberg, Geochemical characterization of groundwater flow in the Santa Fe Group aquifer system, Middle Rio Grande Basin, New Mexico, *U.S. Geol. Surv. Water-Resour. Invest. Rep. 03-4131*, in press, 2004.

Poeter, E. P., and M. C. Hill, Documentation of UCODE, a computer code for universal inverse modeling, *U. S. Geol. Surv. Water-Resour. Invest. Rep. 98-4080*, 116 pp., 1998.

Pollock, D. W., User's guide for MODPATH/MODPATH-PLOT, version 3: A particle tracking post-processing package for MODFLOW, the U. S. Geological Survey finite-difference ground-water flow model, *U. S. Geol. Surv. Open-File Rep. 94-464*, variously paged, 1994.

Polyak, V. J., J. C. Cokendolpher, R. A. Norton, Y. Asmerom, Wetter and cooler late Holocene climate in the southwestern United States from mites preserved in stalagmites, *Geology, 29*, 643-646, 2001.

Reeder, H. O., L. J. Bjorklund, and G. A. Dinwiddie, Quantitative analysis of water resources in the Albuquerque area, New Mexico—Computed effects on the Rio Grande of pumpage of ground water, 1960-2000, *New Mexico State Engineer Tech. Rep. 33,* 34 pp., 1967.

Reiter, M., Using precision temperature logs to estimate horizontal and vertical groundwater flow components, *Water Resour. Res. 37*, 663-674, 2001.

Sanford, W. E., L. N. Plummer, and L. M. Bexfield, Using environmental tracer data to improve the U. S. Geological Survey MODFLOW model of the Middle Rio Grande Basin, in *U. S. Geological Survey Middle Rio Grande Basin Study—Proceedings of the second Annual Workshop, Albuquerque, New Mexico, February 10-11, 1998*, edited by J. L. Slate, pp. 13-14, *U. S. Geol. Surv. Open-File Rep. 98-337*, 1998.

Sanford, W. E., L. N. Plummer, D. P. McAda, L. M. Bexfield, and S. K. Anderholm, Estimation of hydrologic parameters for the ground-water model of the Middle Rio Grande Basin using carbon-14 and water-level data, in *U. S. Geological Survey Middle Rio Grande Basin Study—Proceedings of the Fourth Annual Workshop, Albuquerque, New Mexico, February 15-16, 2000,* edited by J. C. Cole, pp. 4-6, *U. S. Geol. Surv. Open-File Rep. 00-488*, 2001.

Sanford, W. E., L. N. Plummer, D. P. McAda, L. M. Bexfield, and S. K. Anderholm, Use of environmental tracers to estimate parameters for a predevelopment-ground-water-flow model of the Middle Rio Grande Basin, New Mexico, *U.S. Geol. Surv. Water-Resour. Invest. Rep. 03-4286,* in press, 2004.

Stone, B. D., B. D. Allen, M. Mikolas, J. W. Hawley, W. C. Haneberg, P. S. Johnson, B. Allred, and C. R. Thorn, Preliminary lithostratigraphy, interpreted geophysical logs, and hydrogeologic characteristics of the 98th Street core hole,

Albuquerque, New Mexico, *U.S. Geol. Surv. Open-File Rep. 98-210*, 82 pp., 1998.

Stute, M., P. Schlosser, J. F. Clark, and W. S. Broecker, Paleotemperatures in the southwestern United States derived from noble gases in ground water, *Science, 256*, 1000-1003, 1992.

Stute, M., J. F. Clark, P. Schlosser, W. S. Broecker, and G. Bonani, A 30,000 yr continental paleotemperature record derived from noble gases dissolved in groundwater from the San Juan Basin, New Mexico, *Quatern. Res., 43*, 209-220, 1995.

Stute, M., and P. Schlosser, Atmospheric noble gases, in *Environmental Tracers in Subsurface Hydrology,* edited by P. Cook, and A. Herczeg, pp. 349-377, Kluwer Academic Press, Amsterdam, 1999.

Thompson, R. S., K. H. Anderson, and P. J. Bartlein, Quantitative paleoclimatic reconstructions from late Pleistocene plant macrofossils of the Yucca Mountain Region, *U.S. Geol. Surv. Open-File Rep. 99-338*, 38 pp., 1999.

Thorn, C. R., D. P. McAda, and J. M. Kernodle, Geohydrologic framework and hydrologic conditions in the Albuquerque Basin, central New Mexico, *U.S. Geol. Surv. Water-Resour. Invest. Rep. 93-4149*, 106 pp., 1993.

Tiedeman, C. R., J. M. Kernodle, and D. P. McAda, Application of nonlinear-regression methods to a ground-water flow model of the Albuquerque Basin, New Mexico, *U.S. Geol. Surv. Water-Resour. Invest. Rep. 98-4172*, 90 pp., 1998.

Titus, F. B., Ground-water geology of the Rio Grande trough in north-central New Mexico, with sections on the Jemez Caldera and Lucero Uplift, in *Guidebook of the Albuquerque country,* edited by S. A. Northrop, pp. 186-192, *New Mexico Geol. Soc., 12th Field Conf.*, 1961.

Straaten, C. van der, and W. G. Mook, Stable isotopic composition of precipitation and climatic variability, in *Palaeoclimates and Palaeowaters: A Collection of Environmental Isotope Studies,* International Atomic Energy Agency, pp. 53-64, Vienna, Austria, 1983.

Vuataz, F. D., and F. Goff, Isotope geochemistry of thermal and nonthermal waters in the Valles Caldera, Jemez Mountains, northern New Mexico, *J. Geophys. Res. 91*, 1835-1853, 1986.

Wilkins, D. E., and D. R. Currey, Timing and extent of late Quaternary paleolakes in the Trans-Pecos closed basin, west Texas and south-central New Mexico, *Quatern. Res. 47*, 306-315, 1997.

Yapp, C. J., D/H variations of meteoric waters in Albuquerque, New Mexico, U.S.A., *J. Hydrol. 76*, 63-84, 1985.

S.K. Anderholm and L.M. Bexfield, U.S. Geological Survey, 5338 Montgomery, NE, Suite 400, Albuquerque, New Mexico 87109.

E. Busenberg and L.N. Plummer, U.S. Geological Survey, 432 National Center, Reston, Virginia 20192.

W.E. Sanford, U.S. Geological Survey, 431 National Center, Reston, Virginia 20192.